University of Missouri-Rolla

Electromagnetic Compatibility Laboratory

Title: **The Effects of Wire Radius on a Simple Electronic Circuit Acting as a Small Loop Antenna**

Report Number: TR91-3-003

Author: John Rowland

Date: May 8, 1991

THE EFFECTS OF WIRE RADIUS ON A SIMPLE ELECTRONIC CIRCUIT ACTING AS A SMALL LOOP ANTENNA

By: John B. Rowland

Presented To: Dr. T. H. Hubing

EE - Dept.
EE - 300

May 8, 1991

ABSTRACT

Given a small electronic circuit, which besides performing its intended function may act as a small loop antenna. The maximum E-field strength can be calculated using:

$$|E|_{max}(R<\eta_o) = \frac{V\Delta S\eta_o\beta^2}{4\pi rR}$$

$$|E|_{max}(R>\eta_o) = \frac{V\Delta S\eta_o\beta^2}{4\pi r} \qquad \text{EQ(1)}$$

But these equations give only a constant E-field value and do not take into account the effects of loop inductance as a function of wire radius. Incorporating a variable into EQ(1), to account for a change in wire radius, improves the accuracy of the results and provides a more accurate accounting of the behavior of the circuit as a loop antenna. This study explores this phenomena in detail and introduces a change to EQ(1) to include a variable for a change in wire radius.

TABLE OF CONTENTS

INTRODUCTION

As electromagnetic interference becomes more at issue in today's world, closer attention must be paid to unintentional radiators. One of the many unintentional radiators in this technological environment is the simple circuit given in figure #1:

FIGURE #1

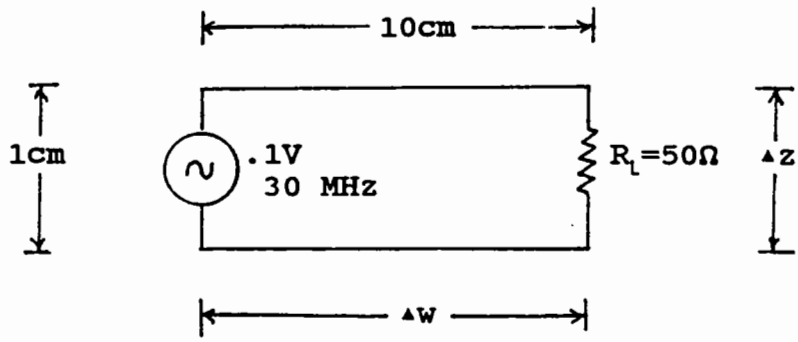

This is a simple electronic circuit configuration which may appear on any printed circuit board, however most circuits have smaller dimensions when placed on the printed circuit board. Although a simple electronic circuit, it is also a small loop antenna. This simple circuit, while performing its intended functions, is also radiating electromagnetic waves which may cause interference in another nearby circuit. A barometer as to the efficiency of the loop antenna in figure #1, as a radiator, is the radiated electric field (E-field) strength.

In the far field (approximated by r >> Lambda), the magnitude of the E-field strength can be approximated by:[1]

$$|E|_{max}(R<\eta_o) = \frac{V\Delta S\eta_o\beta^2}{4\pi rR}$$

EQ(1)

$$|E|_{max}(R>\eta_o) = \frac{V\Delta S\eta_o\beta^2}{4\pi r}$$

But, this configuration has some inherent shortcomings which may lead to inaccurate results. This approximation does not take into account the effects of loop inductance due to the changes in wire radius, the inefficiency of the loop as a radiator as the wire diameter increases, and changes in the shape of the circuit. The model using EQ(1) assumes an infinitely small wire radius, the current is regulated by V/R_L, and the shape of the loop unaffects the radiation pattern and thus the E-field strength. The object of this study is to rewrite EQ(1) such that as much error as possible is eliminated and to improve the accuracy of the calculated results.

To achieve the objective, EQ(1) was rewritten to account for changes in wire radius, but not loop shape. To account for loop shape would be a difficult task, to say the least. Additionally, where the loop becomes an inefficient radiator, as the wire diameter closes the distance Δz (see figure #1), is not accounted for. Wires with large diameters relative to the loop size, become poor radiators. In general, loop antennas can become more efficient as wire radius increases. From Constantine A. Balanis' **Antenna Theory**, equation #5-24:

$$R_r = 20\pi^2\left(\frac{C}{\lambda}\right)^4$$

and equation #2-86b:

$$R_L = \frac{b}{a}\sqrt{\frac{\omega\mu_o}{2\sigma}}$$

and equation #2.86:

$$e = \frac{R_L}{R_r + R_L}$$

where:[2]

e = The loop antenna radiation efficiency
a = The loop wire radius
b = The loop radius

As seen with the equation defining radiation efficiency of the loop antenna, as the wire radius increases, R_L approaches zero and the efficiency to one. This is practically not feasible. The loop antenna in figure #1 becomes less efficient at the higher radius values. This probably has more to do with the shape of the loop than anything else. This phenomena was not explored in the model or by experimentation. Generally speaking, circuits on printed circuit boards use wires very small compared to the loop size. If the geometry is correct, the circuit could become a rather efficient loop radiator causing considerable interference.

MODELLING WITH NEC

The small circuit in figure #1 was first modelled as an antenna using the Numerical Electromagnetics Code, NEC, developed

by Lawrence Livermore Laboratories. This was done to obtain as accurate a baseline model as possible. The NEC program calculates such parameters as radiation patterns, input impedance, Z_{in}, and the far field E-field strength.[3] Using NEC, plots of the antenna input admittance (Y_{in}) and far field E-field strength, as a function of wire radius, was obtained. Input admittance was plotted as it gives a representation of the current through the loop. Because $I = V*Y_{in}$, the voltage source is simply a scaling factor as curve behavior is of primary interest. Figure #2a and #2b shows the plots of the E-field strength and input admittance for the circuit in figure #1. In Appendix A, plots of input admittances and E-field strengths are given for different values of load resistance.

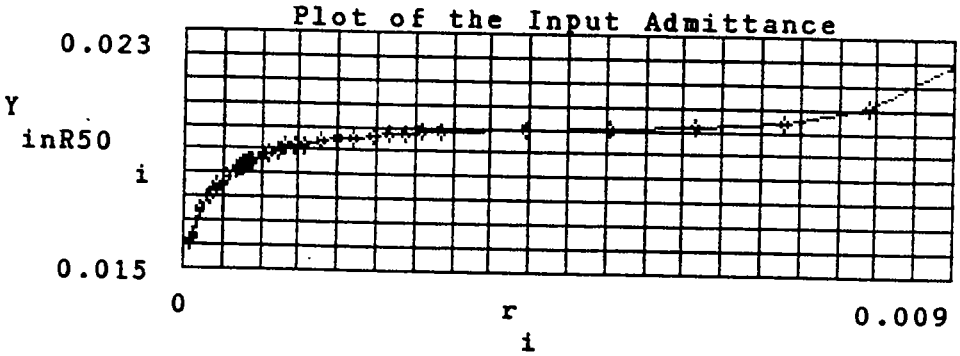

FIGURE #2a

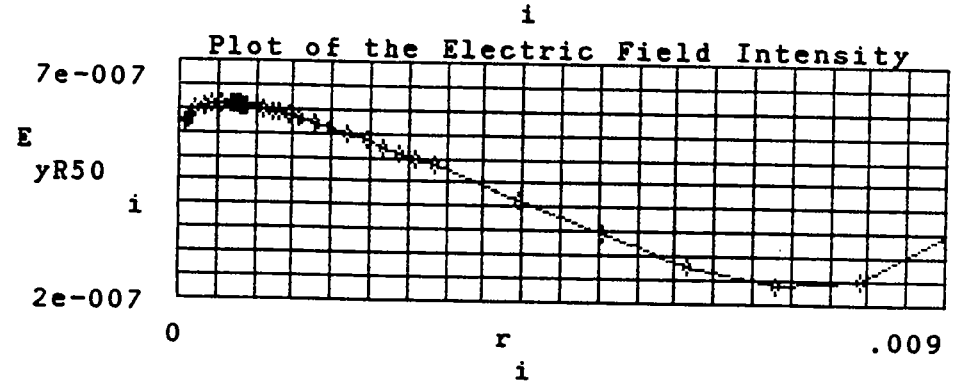

FIGURE #2b

Figure #2a illustrates how as wire radius increases, the current increases sharply, levels off, and then rises sharply again. This is explained with the aid of figure #3 below:

FIGURE #3

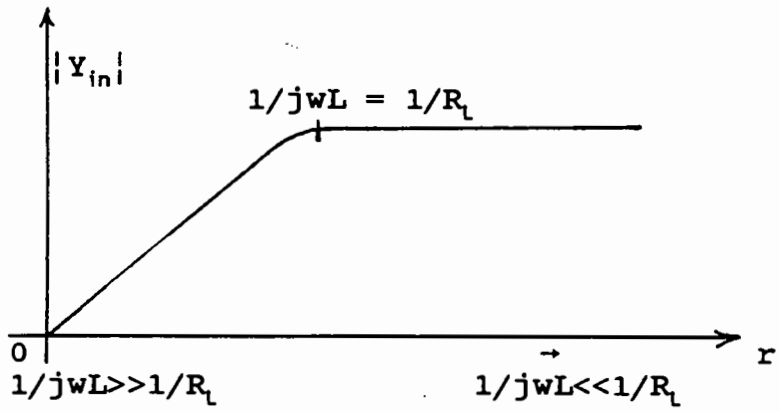

The plots in figure #2 and #3 have wire radius ranges inclusive of .00009m to .009m (.00009m < r < .009m). EQ(1) assumes the current is limited by V/R_L. If this were the case, the loop current in figure #2a would be a constant value governed, again by V/R_L. But as can be seen in figure #3, there is an increase in current, from a very small value, to its final value governed by $1/R_L$. The gradual change from 0 to $1/R_L$ is due to the contributions of loop inductance, jwL. Where the wire radius is very small, the loop inductance is great and dominating control over the current. The contributions to control over the current by $1/R_L$ at this point is negligible ($1/jwl >> 1/R_L$). As wire radius increases, loop inductance starts to level off and its contribution to control over the current decreases. This occurs at the point where the loop inductance equals the load resistance ($1/jwL = 1/R_L$) resulting in a break or knee. From this break point onward, in the

direction of increasing wire radius, the control of the current is regulated by the value of $1/R_L$. The contribution by 1/jwL is now negligible ($1/jwL >> 1/R_L$). The plot in figure #2a bears this out.

The rise in the current at the higher radius values is the result of a capacitive coupling effect. As the wire radius increases, such that the distance between the wires is much less than Δz and where they are nearly touching, capacitive coupling occurs causing a short in the loop. This phenomena is illustrated by figure #4.

FIGURE #4

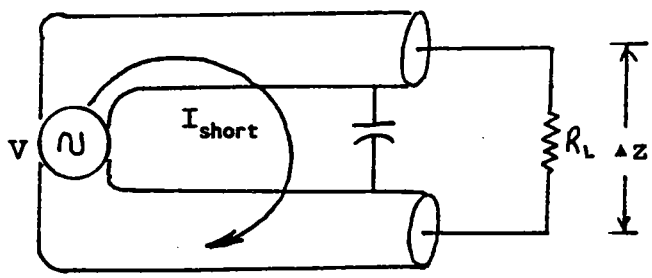

At this point, the effective area of the loop is small enough such that the effects of loop inductance are not effective and thus do not offer any control over the current through the loop. In the standard loop antenna, the loop inductance impedes the flow of current through the loop. The expression for the input impedance to the circuit in figure #1 is $Z_{in} = R_L + jwL$. R_L is the value of the load resistance and jwL is the value of the loop inductance.

The E-field plot in figure #2b gives the maximum E-field strength as a function of wire radius. To ensure only the far field E-field components were calculated, the fields were calculated at a distance of thirty meters. EQ(1) is a far field ex-

pression and does not account for the changes in the radiated fields due to near field effects when used to measure E-field strengths in the near field. Calculations were made in the x-direction resulting in the maximum E-field strength in the y-direction, as given by the Poynting Vector. Figure #2b shows an increasing E-field as current increases. The peak E-field values do not correspond with the peak current values as related to wire radius, where the loop susceptance equals the load conductance ($1/jwL = 1/R_L$). The peak in figure #2 occurs at r = .0006m. The drop off in the E-field strength is due to the irregular geometry of the loop and the large wire diameters relative to the loop size. This can be seen in figure #5 below:

FIGURE #5

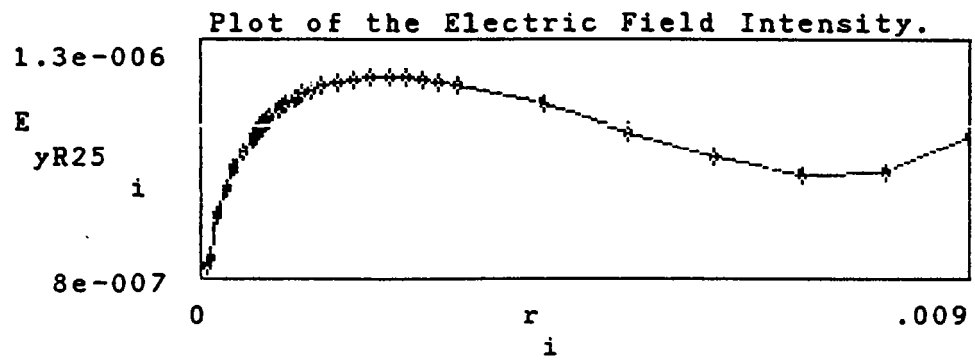

As the value of the load resistance is changed, the peak of the E-field strength does, as well. With the value of R_L decreased to 25Ω, the peaks increased to a higher corresponding value of wire radius. Greater values of R_L have the same effect, but in the reverse direction. Decreasing the value of R_L by half doubles the break point from the origin. The reverse is true if the value of R_L is doubled.

FIGURE #6

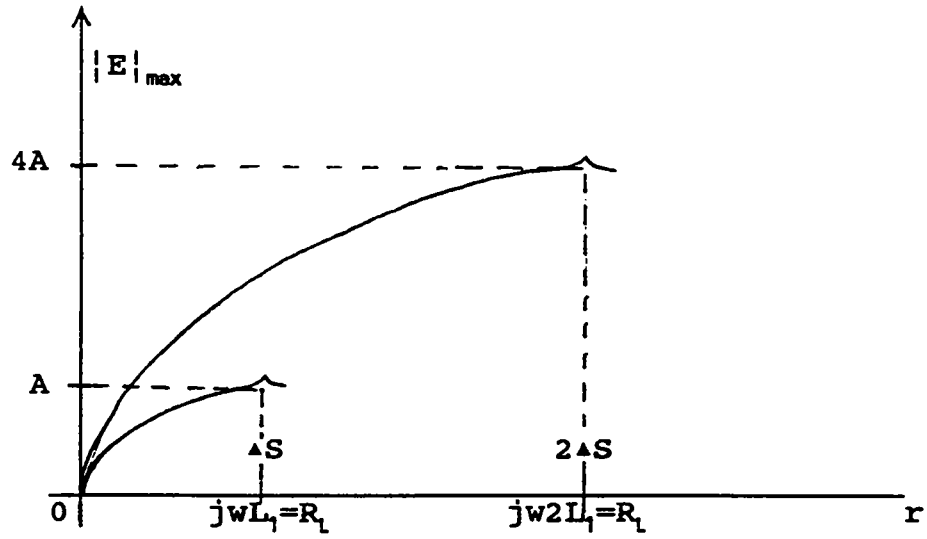

It should be noted that if ▲S were doubled the E-field would quadruple in strength. But, the break point would be further down the path of increasing wire radius. Because the loop area has been doubled, the loop inductance increased by approximately the same amount. Loop inductance can be approximated by loop area. The magnitude of the E-field is increased, or decreased, by the square of the factor multiplied to ▲S. Thus the old, as well as the new formulas account for changes in the overall size of the loop.

NEC analysis was performed on circuits with values of R_L equal to 25Ω, 50Ω, 100Ω, 1 KΩ, and 10 KΩ. This analysis lead to a series of curves which can be divided into two categories. These curves are given in figure #7 below:

FIGURE #7

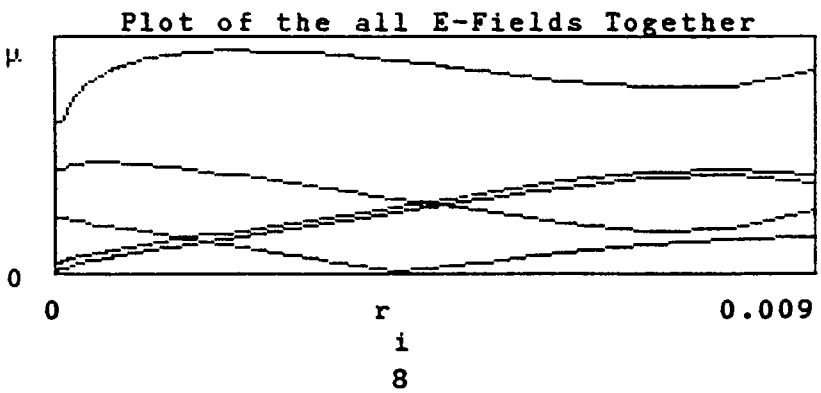

Separation of the two sets of curves occurs a 377Ω, the intrinsic impedance of free space. But why a difference in the behavior of the two curves? It was determined that the curves related to values of R_L greater than 377Ω, especially much greater than 377Ω, were characteristic of the loop antenna's dual, the magnetic dipole. It was found that load resistance values of 1 KΩ or greater tend to make the loop appear electrically open ended, as in figure #8 below. However, theoretically, the crossover point where the loop antenna behaves as a magnetic dipole should occur at 377Ω. Values of R_L slightly greater than 377Ω were not modelled using NEC.

FIGURE #8

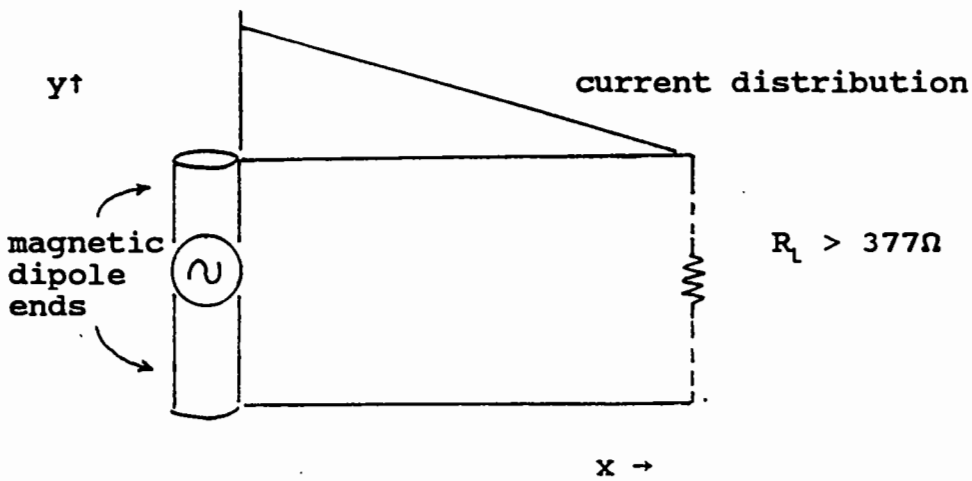

The short stubs along the y-axis are the magnetic dipole ends, while the extra lead lengths along the x-axis carry a decreasing current distribution and do not contribute to the radiated fields. Because the wire is non-ideal and has some internal resistance, there will be a small I^2R loss. This magnetic dipole is an inefficient radiator because its length is much less than a wavelength. Thin wire dipole antennas of length much less than a

wavelength are poor radiators. As the wire radius increases, the dipole leads become thicker in diameter and, relatively speaking, a more efficient radiator. This is evident in the curves in figure #7. The E-field strength increased as the wire radius increased.

Knowing that changes in wire radius should not be considered negligible, changes to EQ(1) were needed to include a varying wire radius. $|E|_{max}$ is derived from:[4]

$$E_\theta = \frac{I_o \Delta z \eta \beta^2}{4\pi} \sin\theta e^{-jkr} \left[\frac{j}{\beta r} + \frac{1}{(\beta r)^2} - \frac{j}{(\beta r)^3} \right]$$

and

$$E_\phi = \frac{-I_o \Delta S \eta_o \beta^3 \sin\theta e^{-j\beta r}}{4\pi} \left[-\frac{1}{\beta r} + \frac{j}{(\beta r)^2} \right]$$

In the far field, the current I_o is given by V/Z_{in}. With the model based on EQ(1), Z_{in} is equal to R_L. A more exact expression including a variable for wire radius, was needed. Using equation #12-30 from **Engineering Electromagnetics** by William H. Hayt, Jr.,

$$Z_o = \frac{1}{\pi} \sqrt{\frac{\mu_o}{\epsilon_o}} \operatorname{acosh}\left[\frac{d}{2a} \right]$$

and equation #12-26 also from the same book:[5]

$$L_1 = \frac{\mu_o}{\pi} acosh[\frac{d}{2a}]$$

where

d = ▲z
a = wire radius

EQ(1) was then modified to produce a more exact set of equations. The new equations incorporated Z_o and L_{in}. $|E|_{max}$ can now be expressed as:

$$|E|_{max}(R_L > \eta_o) = \frac{V\Delta S\beta^2}{(4r)\, acosh[\frac{\Delta z}{2a}]}$$

EQ(2)

$$|E|_{max}(R_L < \eta_o) = \frac{V\Delta S\eta_o\beta^2}{(4\pi r)\sqrt{R^2 + [2\pi f(\frac{\mu_o}{\pi})\, acosh[\frac{\Delta z}{2a}]]^2}}$$

The developments for EQ(2) are given in detail in Appendix B. EQ(2) now accounts for changes in wire radius for both values of R_L above and below 377Ω.

Next EQ(2) was tested to check the behavior of their curves as a function of wire radius. The NEC model was the established base for comparison. Curves were generated using EQ(2) and compared to the NEC model. For values of R_L greater than 377Ω, the curves generated by EQ(2) followed the NEC model with remarkable exactness. These curves are given in figure #9.

FIGURE #9

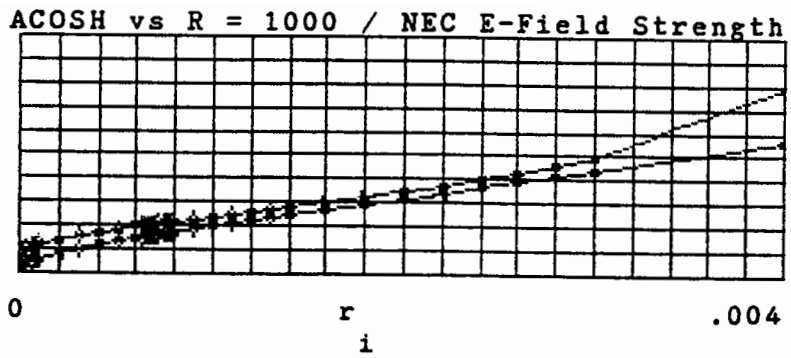

For values of R_L less than 377Ω, the curves generated by EQ(2) are well behaved, in that they track the basic shape of the NEC model. But there is a difference in the peak values. As seen in figure #10, there is an approximate 2.5 dB difference in the values of the E-fields at r=.0005m wire radius.

FIGURE #10

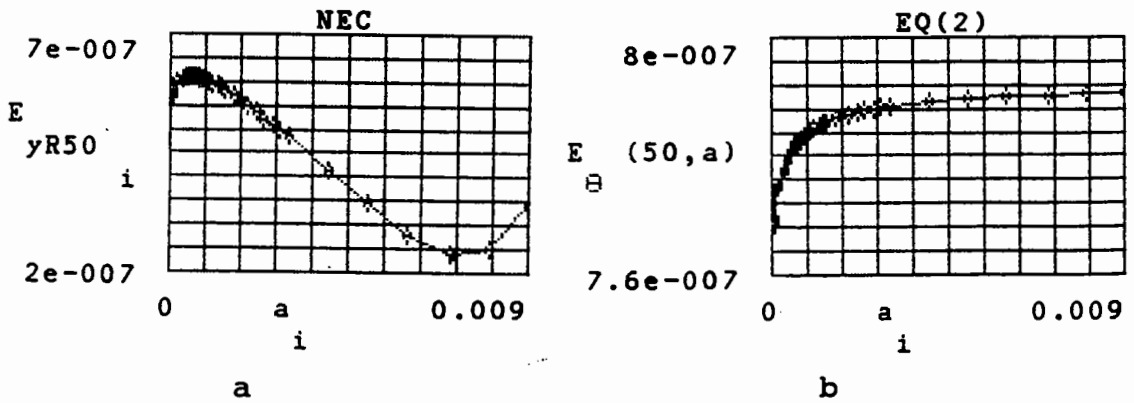

Although not quite as exact as the set of curves EQ(2) generates for values of R_L > 377Ω, the curves related to values of R_L < 377Ω can be considered reasonable.

EXPERIMENTAL TESTING

The next phase of the project was to verify EQ(2) experimentally. Without an anechoic chamber, verification was limited to measuring the input impedance of the loop antenna. With the aid of the HP-8753 Network Analyzer, the reflection coefficient, Γ, was measured. The S_{11} port of the network analyzer measures the reflection coefficient directly. Reflection coefficient is given by:

$$\Gamma=\frac{Z_i-Z_o}{Z_i+Z_o}$$

The network analyzer displays measured data in both magnitude and phase. This results in Γ being a complex number.

Three small loop antennas of radiuses

r = 0.45mm
r = 1.3mm
r = 2.05mm

were molded out of copper wire to the dimensions of the circuit in figure #1.

FIGURE #11

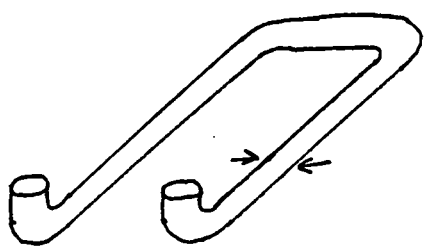

a

None of the antennas could be configured with a load resister, as in figure #1. R_L was approximated by the internal source

resistance of the network analyzer assumed to be 50Ω.

In an attempt to verify EQ(2), using the antenna given in figure #1 and the network analyzer, unreasonable results were obtained. These results were so different from the expected values predicted by NEC, some form of problem in the measurement existed. At the time of this writing, the experimental phase of this study could not be completed. Appendix C gives an accounting of the work done towards the experimental verification.

CONCLUSION

EQ(2) is a more accurate equation taking into account the effects of a changing wire radius. In general a loop antenna becomes more efficient as wire radius increases. The loop antenna in figure #1 became more efficient up to a certain wire radius value and then dropped off despite increasing wire radius. Much of this is probably due to the geometry of the loop. Without having explored this further, loop geometry may prove to be an effective tool to curb unintentional radiation.

For $R_l = 50\Omega$ and a wire radius of r = .0009m:

$$|E|_{EQ(1)} = .78598\ \mu\ V/m$$

$$|E|_{NEC} \approx .6\ \mu\ V/m$$

$$|E|_{EQ(2)} \approx .784\ \mu\ V/m$$

Seemingly, EQ(1) and EQ(2) results are nearly equal, but only in a very small range of wire radiuses. Additionally, while EQ(1)'s value remains constant over the range of wire radiuses, EQ(2)'s value changes due to the effects of loop inductance. Thus EQ(2)'s

ability to predict a more accurate value for $|E|_{max}$ makes it a superior equation to EQ(1). However, the useful range of EQ(2) for $R_L = 50\Omega$ is approximately $.00009m < r < .00027m$. Approximately 2 dB down from the peak E-field value, in the direction of increasing wire radius, was used to determine the range of valid wire radiuses. Similar techniques can be used to find the effective ranges for the other values of R_L given in the respective plots of Appendix A. The usable range of acceptable values given by EQ(2) can vary depending upon the value of R_L. Still, EQ(2) can give acceptable results. EQ(2) can be used as an accurate model to predict the maximum $|E|$-field strength within a limited effective range. In most cases, the wire radius in question should fall within an acceptable range of values.

APPENDIX A

PLOTS

Plots of the magnatudes of the electric field, |Ey|, [at a distance of 30 meters (r = 30m)] and the input admittance of the antenna, |Yin|, calculatedover a range of wire radiuses.

There are three plots and a table of data listing the various radiuses at which |Ey| and |Yin| where tested. The three plots will consist of:

A. |Ey| vs. radius
B. |Ey| vs. radius
C. |Yin| vs. radius

DATA:

$i := 0 \ldots 36 \qquad \mu \equiv 1 \cdot 10^{-6}$

i	r := i	EyR25 := i	YinR25 := i
0	.00009	.83069·μ	.0219573
1	.0001	.84339·μ	.02231873
2	.0002	.93391·μ	.02494485
3	.0003	.99207·μ	.026692786
4	.0004	1.035·μ	.02602765
5	.0005	1.0687·μ	.029113166
6	.0006	1.096·μ	.030026865
7	.00062	1.1008·μ	.0301932
8	.00064	1.1055·μ	.0303551
9	.00066	1.11·μ	.030512287
10	.00068	1.1144·μ	.030664867
11	.0007	1.1186·μ	.030813773
12	.00072	1.1226·μ	.0309583896
13	.00074	1.1265·μ	.0310992899
14	.00076	1.1303·μ	.03123671
15	.00078	1.1339·μ	.03137061
16	.0008	1.1374·μ	.031501283
17	.0009	1.1533·μ	.03210903
18	.001	1.1666·μ	.03265063
19	.0011	1.1779·μ	.033136712
20	.0012	1.1873·μ	.033575087
21	.0013	1.1952·μ	.033972511
22	.0014	1.2018·μ	.034334218
23	.0016	1.2115·μ	.034968059
24	.0018	1.2174·μ	.03550313
25	.002	1.2203·μ	.035960128
26	.0022	1.2208·μ	.03635431
27	.0024	1.2193·μ	.036697272
28	.0026	1.2161·μ	.037006257
29	.0028	1.2115·μ	.037263128
30	.003	1.2057·μ	.037498428
31	.004	1.1633·μ	.03835515
32	.005	1.1091·μ	.03888557
33	.006	1.0563·μ	.03923258
34	.007	1.0209·μ	.039538708
35	.008	1.0248·μ	.039925574
36	.009	1.1043·μ	.040774401

Plots of the magnatudes of the electric field, |Ey|, [at a distance of 30 meters (r = 30m)] and the input admittance of the antenna, |Yin|, calculatedover a range of wire radiuses.

There are three plots and a table of data listing the various radiuses at which |Ey| and |Yin| where tested. The three plots will consist of:

A. |Ey| vs. radius
B. |Ey| vs. radius
C. |Yin| vs. radius

DATA:

$i := 0 \ldots 36 \qquad \mu \equiv 1 \cdot 10^{-6}$

i	r := i	E := yR50 i	Y := inR50 i
0	.00009	.57242·μ	.01591308
1	.0001	.57591·μ	.0160936
2	.0002	.59629·μ	.01694697
3	.0003	.60499·μ	.01746529
4	.0004	.60889·μ	.017823795
5	.0005	.61016·μ	.01809365
6	.0006	.60974·μ	.01830683
7	.00062	.60951·μ	.01834439
8	.00064	.60923·μ	.0183804
9	.00066	.60891·μ	.018415247
10	.00068	.60855·μ	.018448713
11	.0007	.60816·μ	.01848102
12	.00072	.60773·μ	.018512082
13	.00074	.60727·μ	.018542145
14	.00076	.60678·μ	.01857108
15	.00078	.60626·μ	.01859919
16	.0008	.60571·μ	.0186263
17	.0009	.60260·μ	.0187497
18	.001	.59897·μ	.018855994
19	.0011	.59491·μ	.018948356
20	.0012	.5905·μ	.01913474
21	.0013	.5855·μ	.019101086
22	.0014	.58085·μ	.0191647759
23	.0016	.57034·μ	.01927341
24	.0018	.55919·μ	.01936202
25	.002	.54752·μ	.01943563
26	.0022	.53544·μ	.01949767
27	.0024	.52299·μ	.019550692
28	.0026	.51023·μ	.01959636
29	.0028	.49718·μ	.01963633
30	.003	.48387·μ	.01967146
31	.004	.4145·μ	.01979 6
32	.005	.34411·μ	.01988867
33	.006	.28123·μ	.01998342
34	.007	.24097·μ	.02016395
35	.008	.24902·μ	.02065386
36	.009	.34432·μ	.022095398

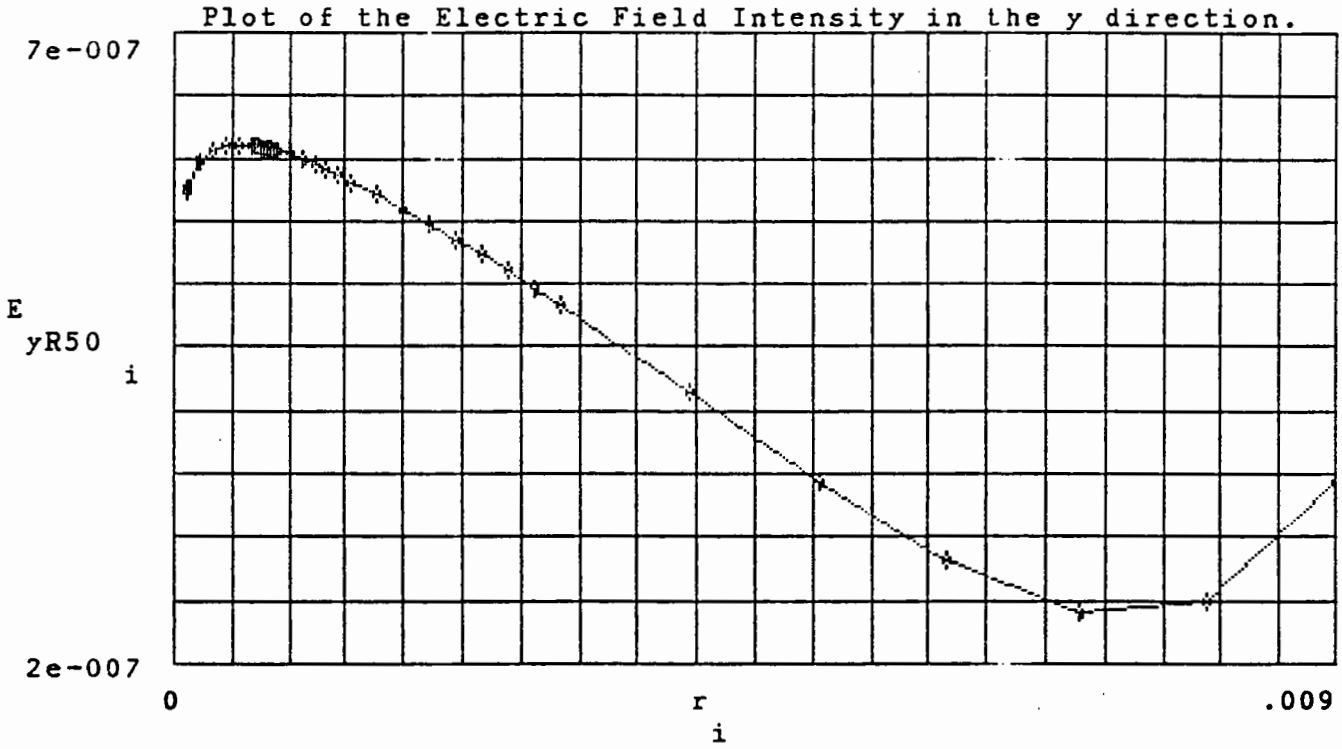

Horozontal Scale = .45 m / div.

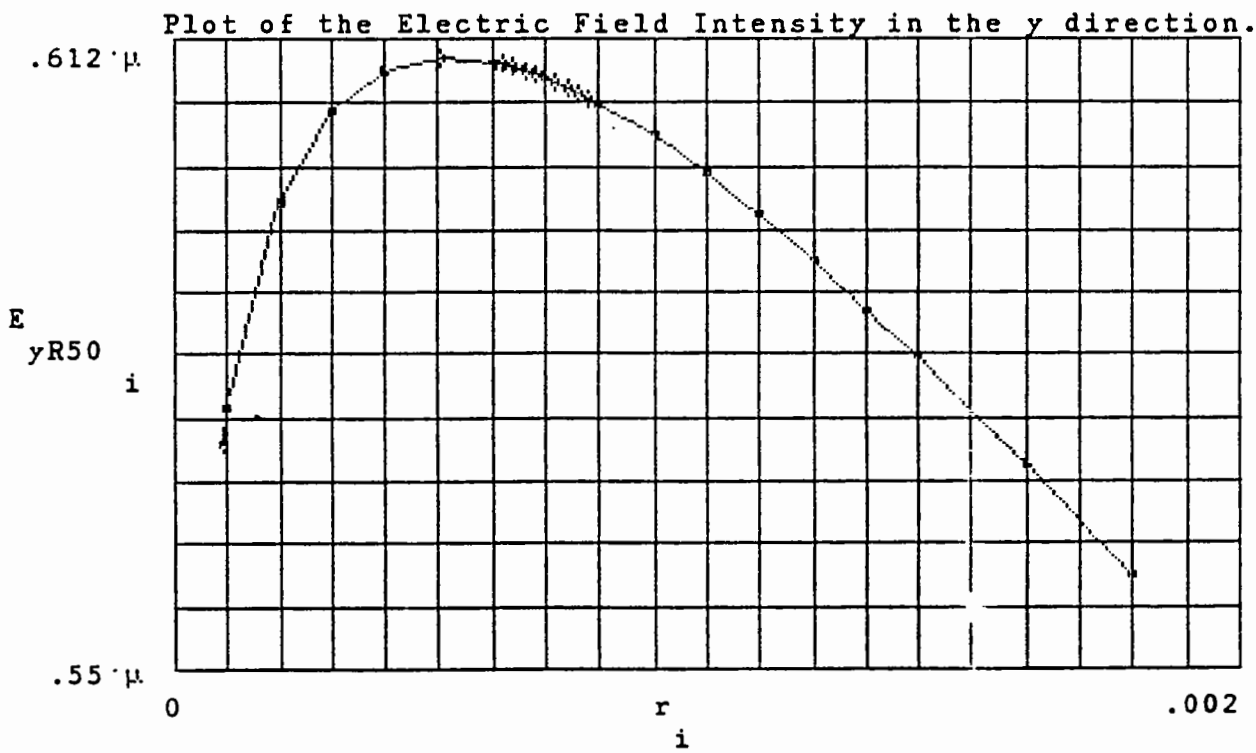

Horozontal Scale = .1 m / div.

Plots of the magnatudes of the electric field, |Ey|, [at a distance of 30 meters (r = 30m)] and the input admittance of the antenna, |Yin|, calculatedover a range of wire radiuses.

There are three plots and a table of data listing the various radiuses at which |Ey| and |Yin| where tested. The three plots will consist of:

A. |Ey| vs. radius
B. |Ey| vs. radius
C. |Yin| vs. radius

DATA:

$i := 0 \ldots 36 \qquad \mu \equiv 1 \cdot 10^{-6}$

i	r := i	E := yR100 i	Y := inR100 i
0	.00009	.30142·μ	.0093464352
1	.0001	.30066·μ	.0093737867
2	.0002	.29277·μ	.0095434647
3	.0003	.28501·μ	.009633452
4	.0004	.27749·μ	.00969258886
5	.0005	.27016·μ	.00973554385
6	.0006	.26296·μ	.009768616
7	.00062	.26153·μ	.009774361
8	.00064	.2601·μ	.00977986457
9	.00066	.25868·μ	.00978514566
10	.00068	.25726·μ	.00979020385
11	.0007	.25584·μ	.00979506855
12	.00072	.25442·μ	.0097997509
13	.00074	.25301·μ	.00980425382
14	.00076	.2516·μ	.009808591
15	.00078	.25019·μ	.0098127781
16	.0008	.24878·μ	.0098168058
17	.0009	.24177·μ	.00983504757
18	.001	.23478·μ	.00985059867
19	.0011	.22782·μ	.00986403
20	.0012	.22087·μ	.00987575974
21	.0013	.21393·μ	.0098861034
22	.0014	.207·μ	.00989528862
23	.0016	.19312·μ	.00991097526
24	.0018	.17925·μ	.0099238862
25	.002	.16534·μ	.00993478463
26	.0022	.15139·μ	.00994419
27	.0024	.13736·μ	.0099524968
28	.0026	.12324·μ	.009959967
29	.0028	.10903·μ	.0099668415
30	.003	.094709·μ	.009973303
31	.004	.021976·μ	.010004793
32	.005	.051433·μ	.010051307
33	.006	.11749·μ	.010157959
34	.007	.16692·μ	.010458967
35	.008	.19148·μ	.011346259
36	.009	.20887·μ	.01378557774

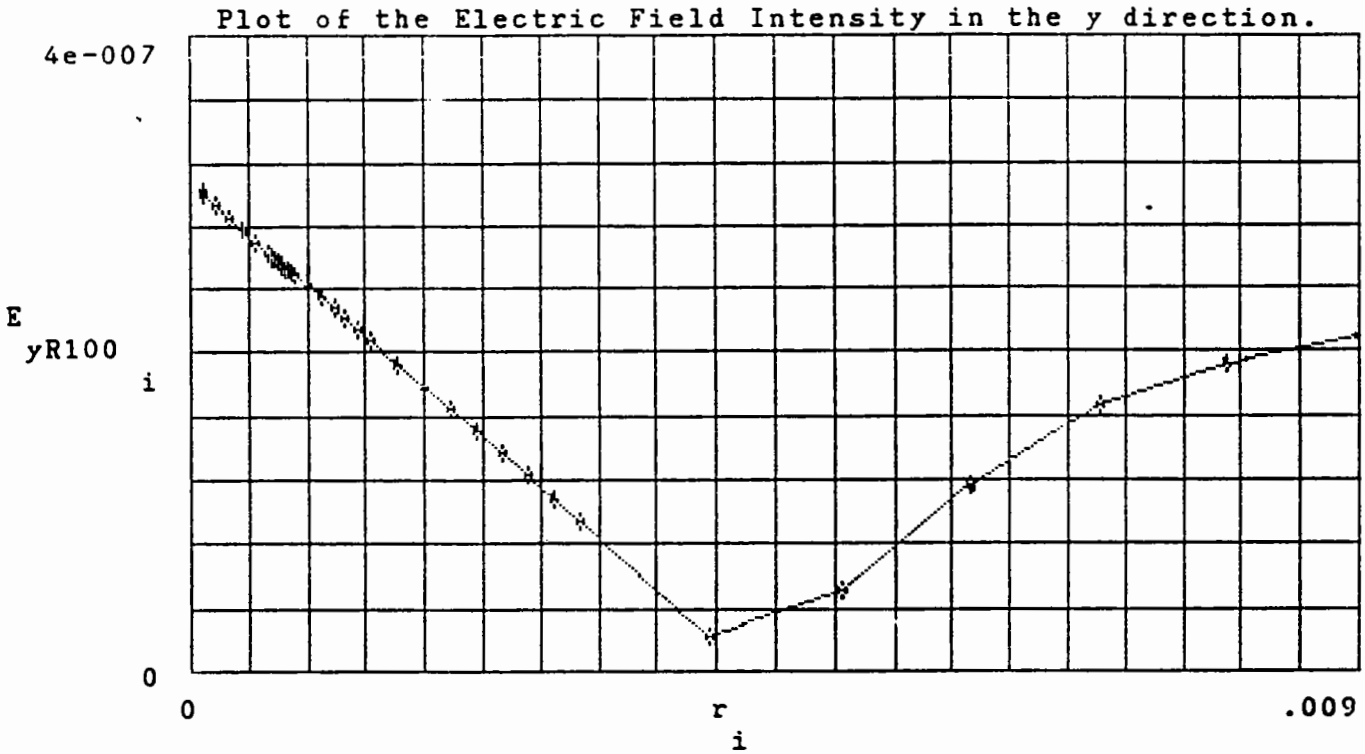

Horozontal Scale = .45 m / div.

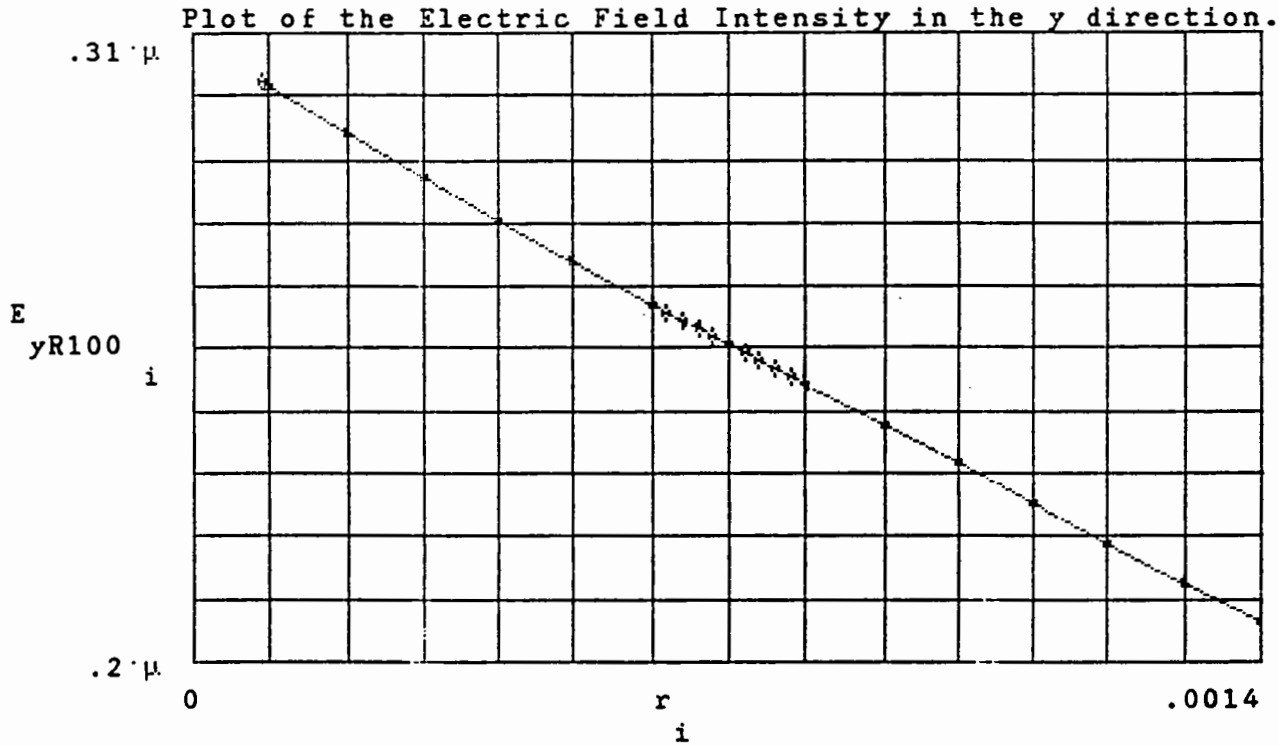

Horozontal Scale = .1 m / div.

DATA:

$i := 0 \ldots 41 \qquad \mu \equiv 1 \cdot 10^{-6}$

r := i
.00001
.00002
.00004
.00006
.00008
.00009
.0001
.0002
.0003
.0004
.0005
.0006
.00062
.00064
.00066
.00068
.0007
.00072
.00074
.00076
.00078
.0008
.0009
.001
.0011
.0012
.0013
.0014
.0016
.0018
.002
.0022
.0024
.0026
.0028
.003
.004
.005
.006
.007
.008
.009

E := yR1000 i
$.010703 \cdot \mu$
$.016393 \cdot \mu$
$.023548 \cdot \mu$
$.028659 \cdot \mu$
$.032826 \cdot \mu$
$.034684 \cdot \mu$
$.036431 \cdot \mu$
$.050399 \cdot \mu$
$.061313 \cdot \mu$
$.070865 \cdot \mu$
$.079655 \cdot \mu$
$.087965 \cdot \mu$
$.089585 \cdot \mu$
$.091193 \cdot \mu$
$.09279 \cdot \mu$
$.094377 \cdot \mu$
$.095955 \cdot \mu$
$.097523 \cdot \mu$
$.099083 \cdot \mu$
$.10064 \cdot \mu$
$.10218 \cdot \mu$
$.10372 \cdot \mu$
$.11132 \cdot \mu$
$.11879 \cdot \mu$
$.12618 \cdot \mu$
$.13348 \cdot \mu$
$.14074 \cdot \mu$
$.14794 \cdot \mu$
$.16277 \cdot \mu$
$.1765 \cdot \mu$
$.19069 \cdot \mu$
$.20489 \cdot \mu$
$.21912 \cdot \mu$
$.2334 \cdot \mu$
$.24777 \cdot \mu$
$.26221 \cdot \mu$
$.33561 \cdot \mu$
$.40862 \cdot \mu$
$.47439 \cdot \mu$
$.52164 \cdot \mu$
$.53585 \cdot \mu$
$.50224 \cdot \mu$

Y := inR1000 i
.0010018682
.001003011
.0010044589
.0010055294
.001006443
.00100685
.001007251
.001010671
.001013688
.001016587
.00101949
.001022447
.001023044
.001236449
.0010242598
.00102487
.001025483
.0010261
.00102674
.00102736
.001027997
.001028635
.0010319065
.0010353084
.00103886
.001042571
.001046449
.00105049
.0010591699
.001068675
.001079111
.001090635
.00110338
.001117555
.001133369
.0011511595
.001283082
.00204205
.002109488
.003254612
.00546924
.009551875

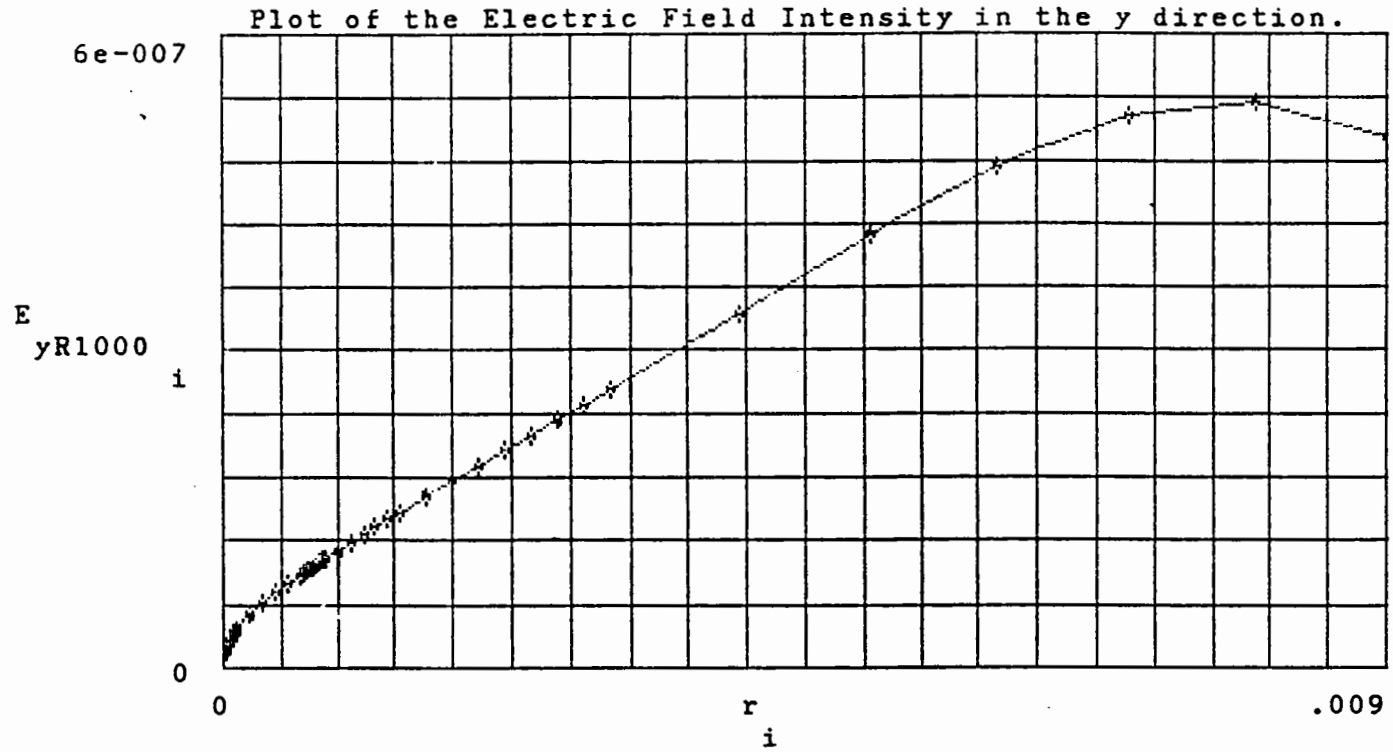

Horozontal Scale = .45 m / div.

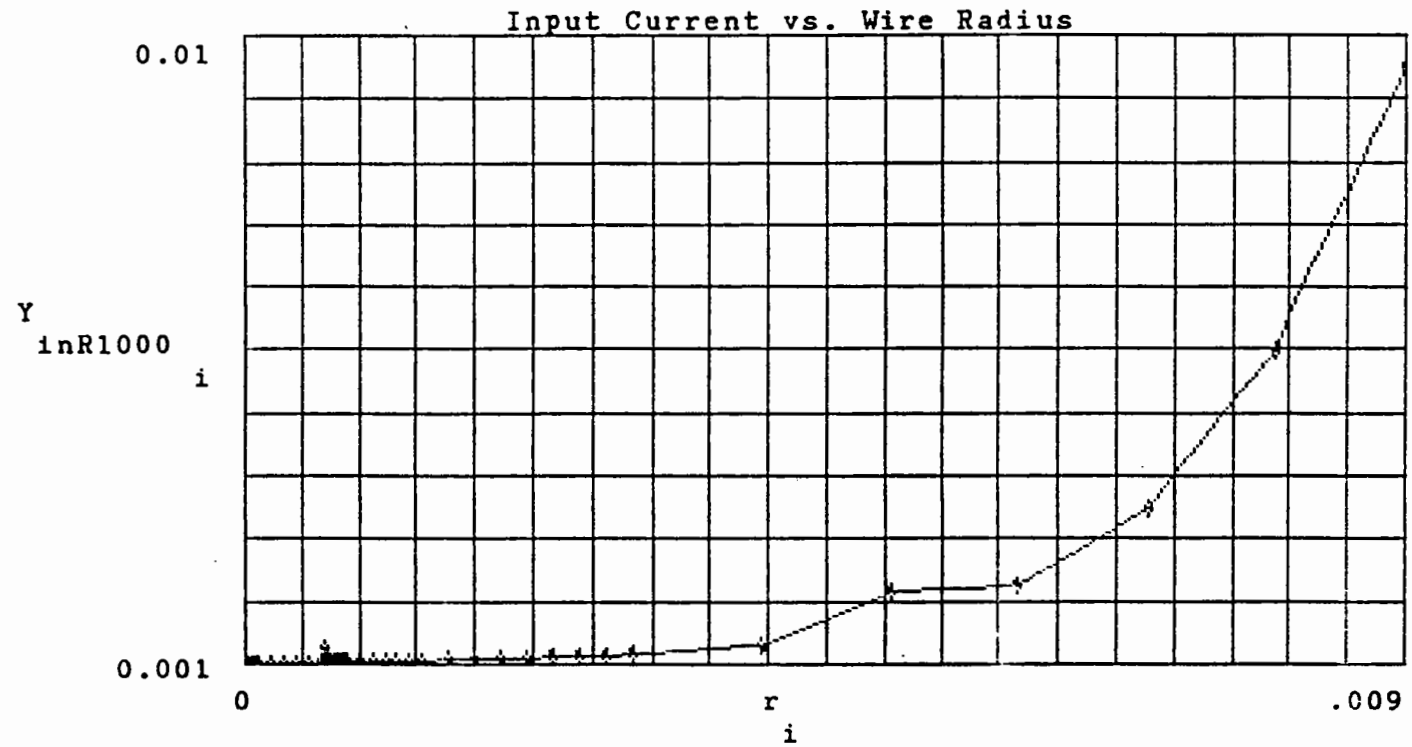

Horozontal Scale = .1 m / div.

Plots of the magnatudes of the electric field, |Ey|, [at a distance of 30 meters (r = 30m)] and the input admittance of the antenna, |Yin|, calculatedover a range of wire radiuses.

There are three plots and a table of data listing the various radiuses at which |Ey| and |Yin| where tested. The three plots will consist of:

A. |Ey| vs. radius
B. |Ey| vs. radius
C. |Yin| vs. radius

DATA:

$m \equiv 1 \cdot 10^{-3}$ $\mu \equiv 1 \cdot 10^{-6}$ $n \equiv 1 \cdot 10^{-9}$ $K \equiv 1 \cdot 10^{3}$

i := 0 ..41

i	r := i	E := yR10000 i	Y := inR10000 i
0	.00001	46.441·n	.130159117·m
1	.00002	52.136·n	.136422·m
2	.00004	59.293·n	.14481027·m
3	.00006	64.406·n	.1511104196·m
4	.00008	68.573·n	.156413022·m
5	.00009	70.432·n	.158823·m
6	.0001	72.178·n	.16111245·m
7	.0002	86.146·n	.18016775·m
8	.0003	97.059·n	.1958486·m
9	.0004	.10661·μ	.2100504·m
10	.0005	.1154·μ	.223466273·m
11	.0006	.12371·μ	.23643237·m
12	.00062	.12533·μ	.238989·m
13	.00064	.12694·μ	.24153784·m
14	.00066	.12853·μ	.24586537·m
15	.00068	.13012·μ	.246616783·m
16	.0007	.1317·μ	.249138434·m
17	.00072	.13327·μ	.25166009·m
18	.00074	.13483·μ	.25417645·m
19	.00076	.13638·μ	.25668914·m
20	.00078	.13792·μ	.259198384·m
21	.0008	.13946·μ	.261704152·m
22	.0009	.14706·μ	.2742077925·m
23	.001	.15454·μ	.286703249·m
24	.0011	.16192·μ	.299232557·m
25	.0012	.16923·μ	.31182768783·m
26	.0013	.17648·μ	.3245147514·m
27	.0014	.18368·μ	.337320237·m
28	.0016	.19801·μ	.36339226595·m
29	.0018	.21224·μ	.39019085838·m
30	.002	.22643·μ	.4179233075·m
31	.0022	.24063·μ	.446803486·m
32	.0024	.25486·μ	.4770681695·m
33	.0026	.26915·μ	.5089871673·m
34	.0028	.28351·μ	.542862825·m
35	.003	.29796·μ	.579039534·m
36	.004	.37136·μ	.8101735595·m
37	.005	.44439·μ	1.1879774·m
38	.006	.51018·μ	1.860121·m
39	.007	.55739·μ	3.0988273·m
40	.008	.57134134·μ	5.378007·m
41	.009	.5362·μ	9.499959·m

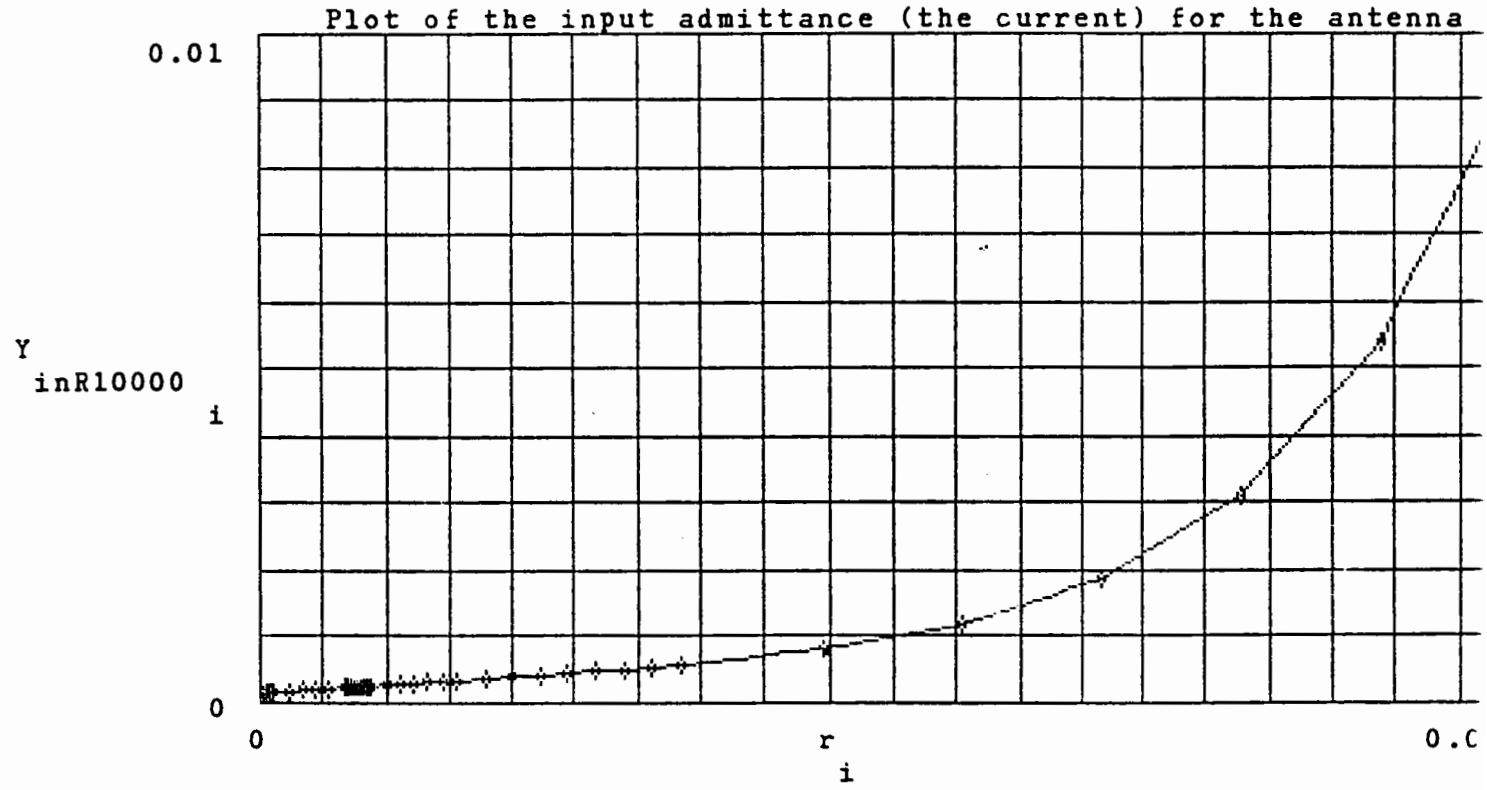

Horozontal Scale = .45 m / div.

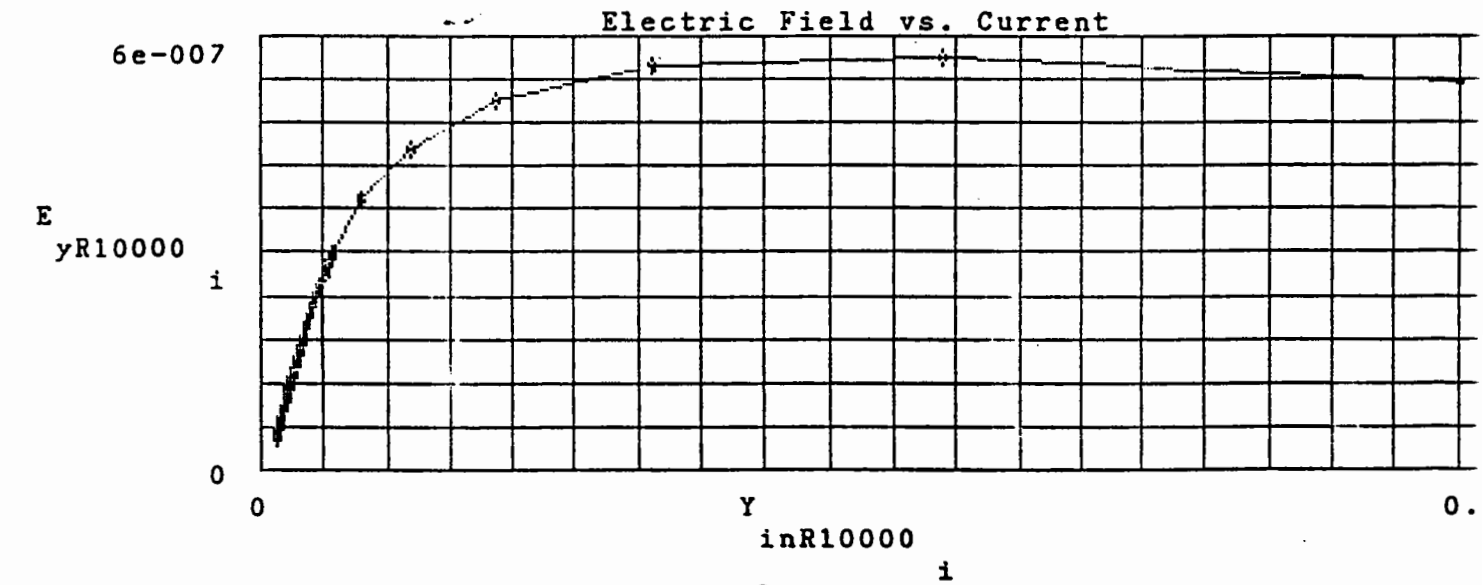

$i := 0 \ldots 36$

$j := 0 \ldots 3$

$f := 1 \cdot 10^{6}$ $\quad \mu \equiv 1 \cdot 10^{-6}$ $\quad \mu_o := 1.256637 \cdot 10^{-6}$

$R_j :=$	$a_i :=$	$E_{yR25_i} :=$	$E_{yR50_i} :=$	$E_{yR100_i} :=$
25	.00009	.83069·μ	.57242·μ	.30142·μ
50	.0001	.84339·μ	.57591·μ	.30066·μ
100	.0002	.93391·μ	.59629·μ	.29277·μ
300	.0003	.99207·μ	.60499·μ	.28501·μ
	.0004	1.035·μ	.60889·μ	.27749·μ
	.0005	1.0687·μ	.61016·μ	.27016·μ
	.0006	1.096·μ	.60974·μ	.26296·μ
	.00062	1.1008·μ	.60951·μ	.26153·μ
	.00064	1.1055·μ	.60923·μ	.2601·μ
	.00066	1.11·μ	.60891·μ	.25868·μ
	.00068	1.1144·μ	.60855·μ	.25726·μ
	.0007	1.1186·μ	.60816·μ	.25584·μ
	.00072	1.1226·μ	.60773·μ	.25442·μ
	.00074	1.1265·μ	.60727·μ	.25301·μ
	.00076	1.1303·μ	.60678·μ	.2516·μ
	.00078	1.1339·μ	.60626·μ	.25019·μ
	.0008	1.1374·μ	.60571·μ	.24878·μ
	.0009	1.1533·μ	.60260·μ	.24177·μ
	.001	1.1666·μ	.59897·μ	.23478·μ
	.0011	1.1779·μ	.59491·μ	.22782·μ
	.0012	1.1873·μ	.5905·μ	.22087·μ
	.0013	1.1952·μ	.5855·μ	.21393·μ
	.0014	1.2018·μ	.58085·μ	.207·μ
	.0016	1.2115·μ	.57034·μ	.19312·μ
	.0018	1.2174·μ	.55919·μ	.17925·μ
	.002	1.2203·μ	.54752·μ	.16534·μ
	.0022	1.2208·μ	.53544·μ	.15139·μ
	.0024	1.2193·μ	.52299·μ	.13736·μ
	.0026	1.2161·μ	.51023·μ	.12324·μ
	.0028	1.2115·μ	.49718·μ	.10903·μ
	.003	1.2057·μ	.48387·μ	.094709·μ
	.004	1.1633·μ	.4145·μ	.021976·μ
	.005	1.1091·μ	.34411·μ	.051433·μ
	.006	1.0563·μ	.28123·μ	.11749·μ
	.007	1.0209·μ	.24097·μ	.16692·μ
	.008	1.0248·μ	.24902·μ	.19148·μ
	.009	1.1043·μ	.34432·μ	.20887·μ

$$E_{\Theta}(R,a) := \left[\frac{.014883}{\sqrt{4 \cdot \pi \cdot 30 \cdot \left[R^2 + \left[2 \cdot \pi \cdot f \cdot \left[\left[\frac{\mu_o}{\pi} \right] \cdot \operatorname{acosh}\left[\frac{.01}{2 \cdot a_i} \right] \right] \right]^2 \right]}} \right]$$

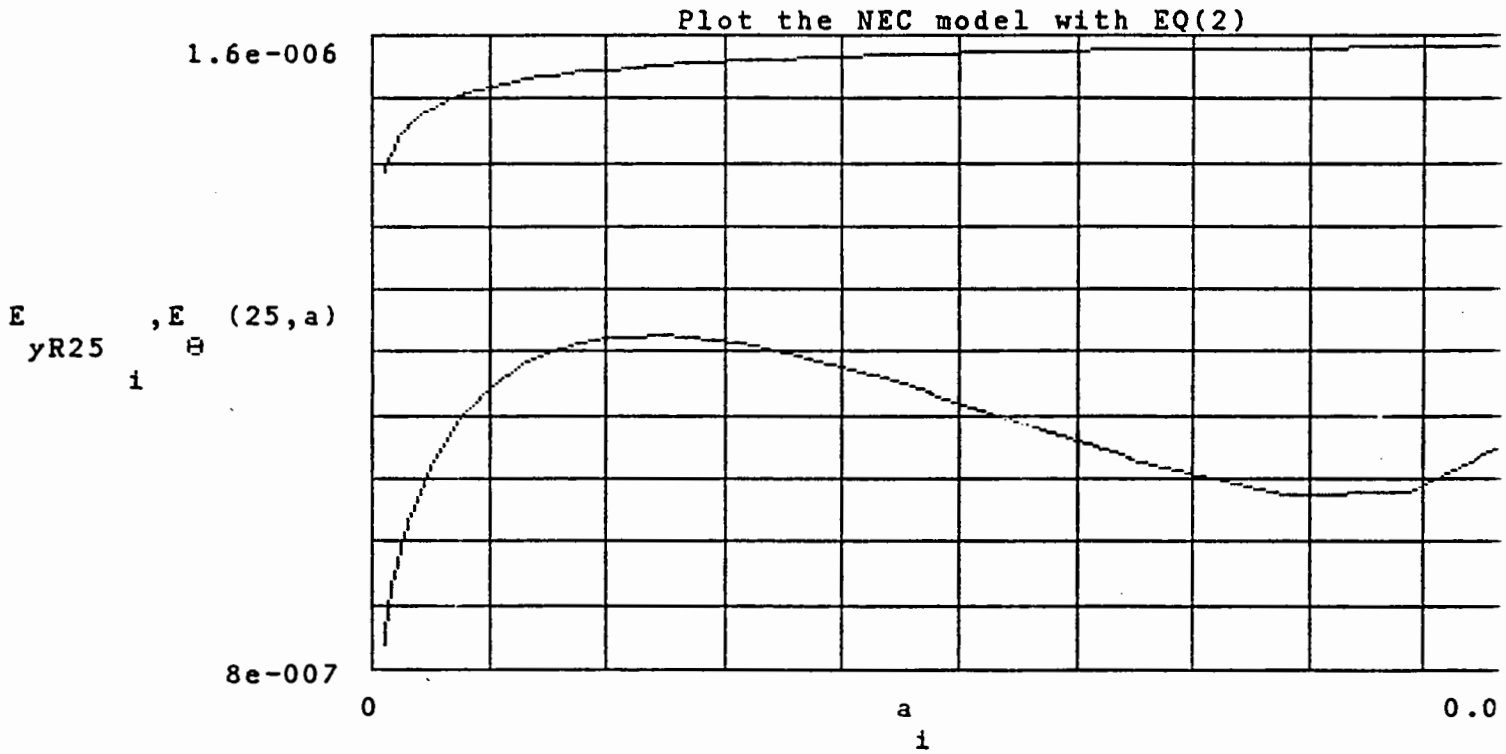

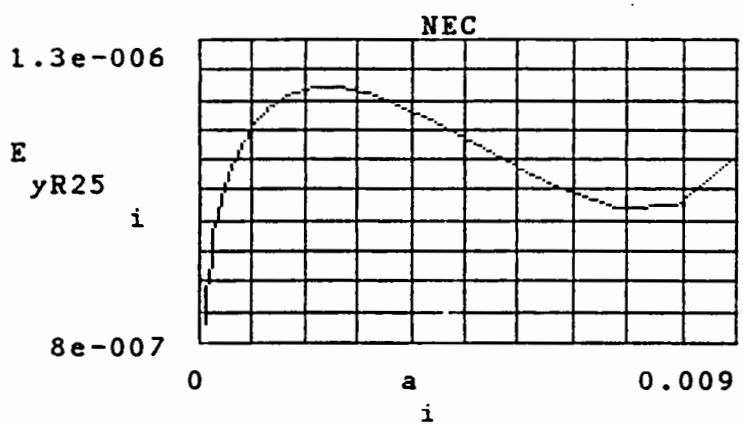

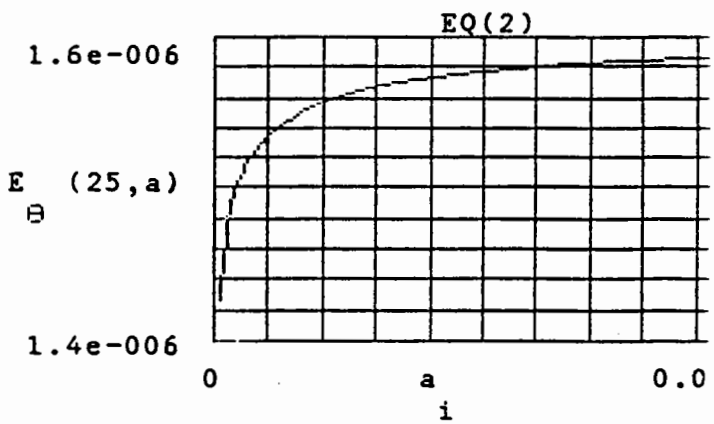

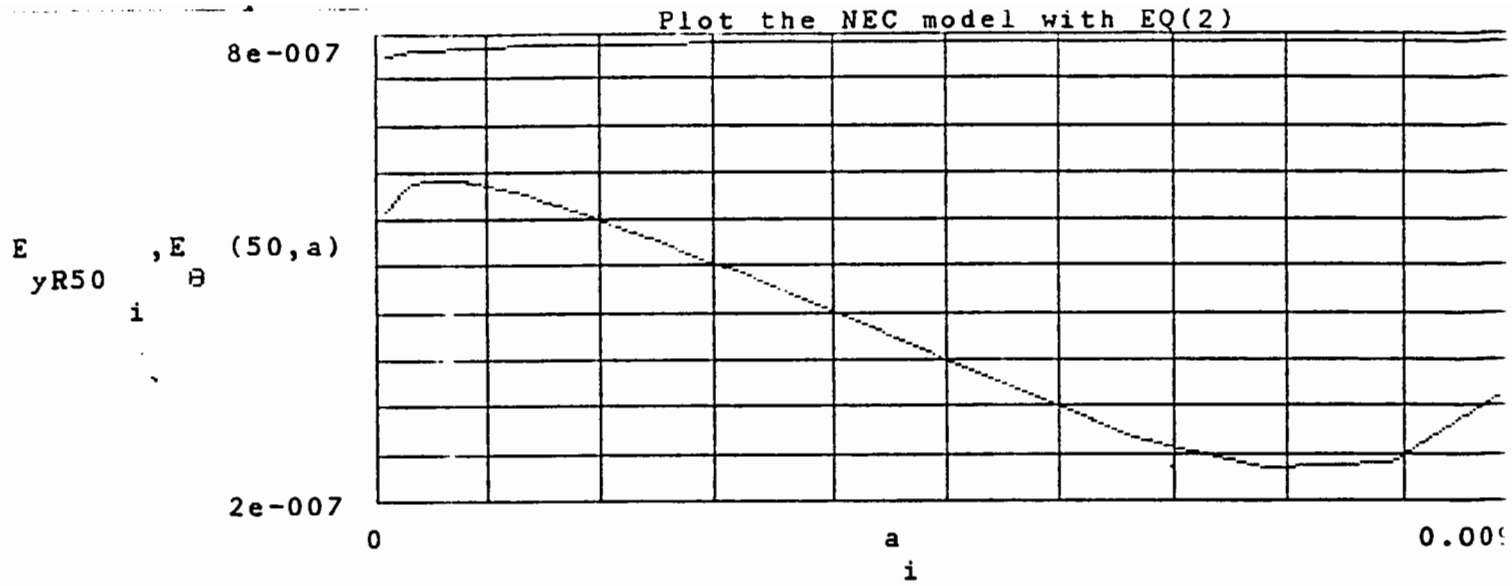
Plot the NEC model with EQ(2)
8e-007
2e-007
E , E (50,a)
yR50 θ
i
0
a
i
0.00

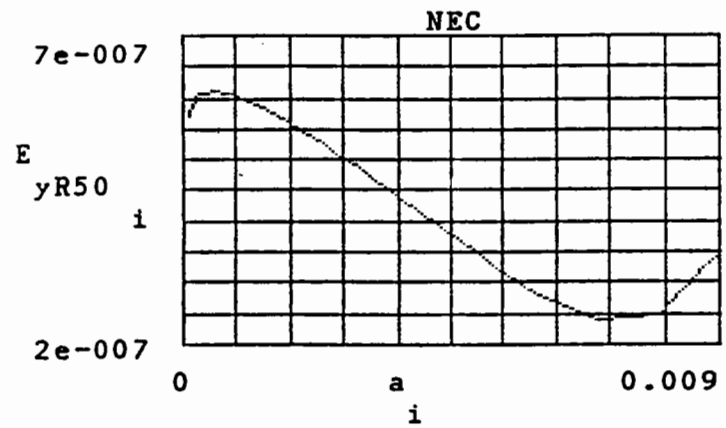
NEC
7e-007
2e-007
E
yR50
i
0
a
i
0.009

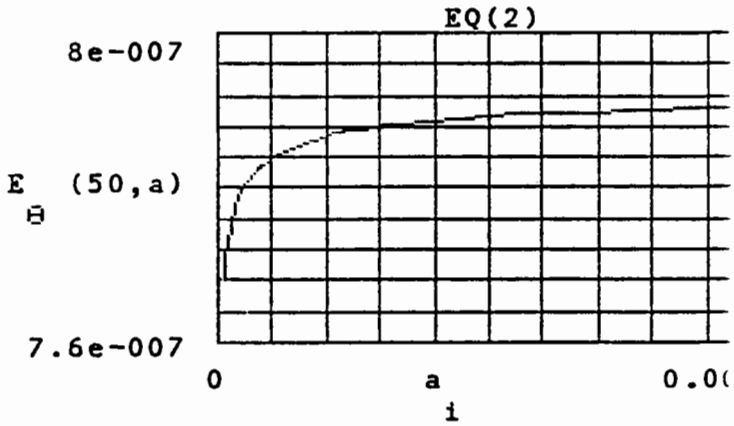
EQ(2)
8e-007
7.6e-007
E (50,a)
θ
0
a
i
0.0

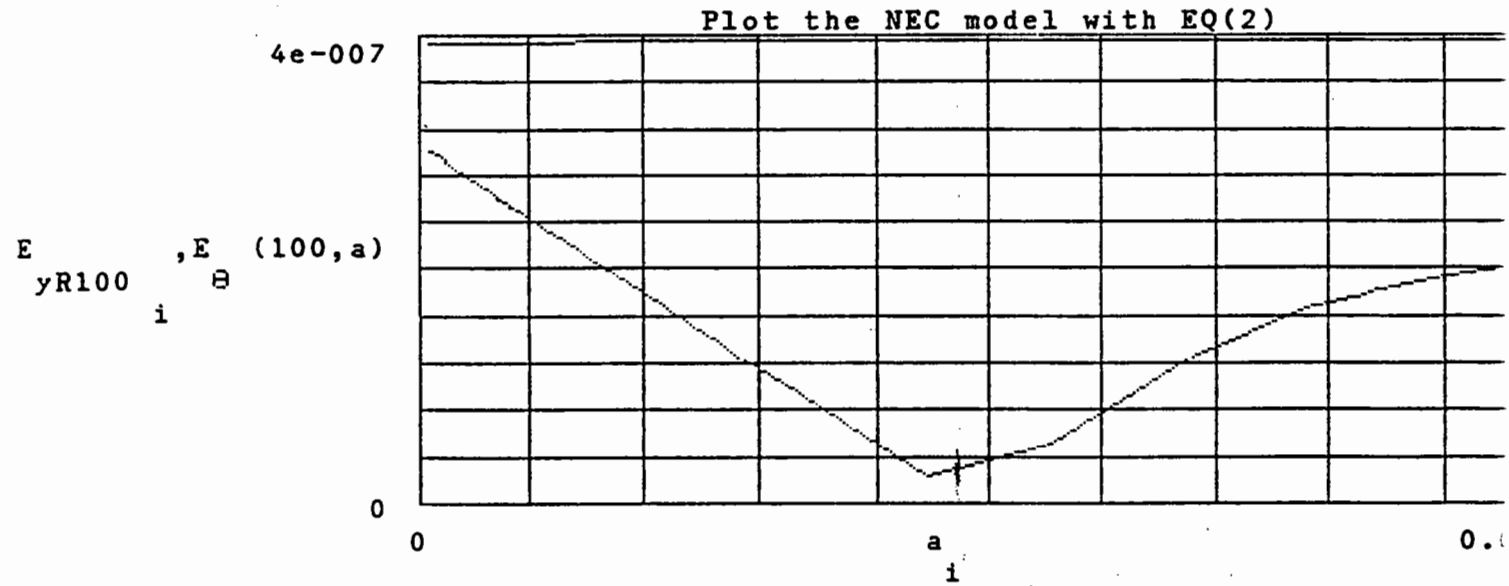
Plot the NEC model with EQ(2)
4e-007
0
E , E (100,a)
yR100 θ
i
0
a
i
0.

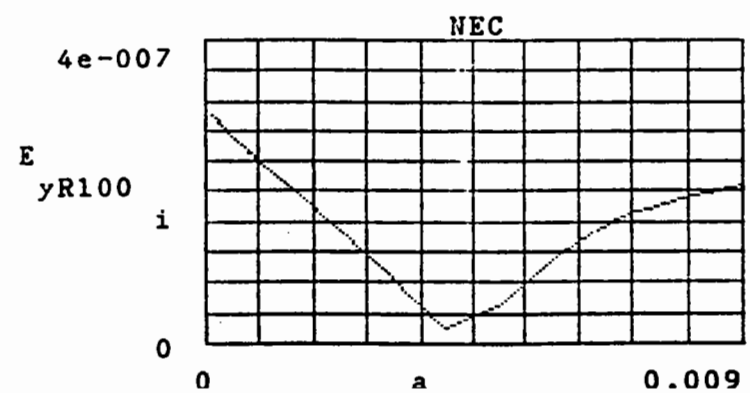
NEC
4e-007
0
E
yR100
i
0
a
0.009

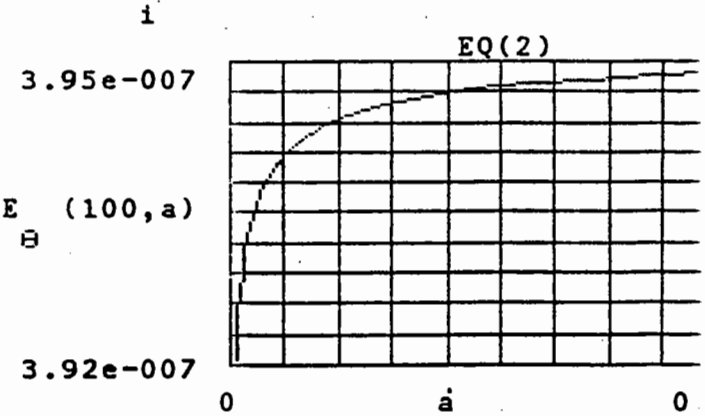
EQ(2)
3.95e-007
3.92e-007
E (100,a)
θ
0
a
0

$i := 1 \ldots 42$ $\quad \mu \equiv 1 \cdot 10^{-6}$ $\quad n \equiv 1 \cdot 10^{-9}$

$r_i :=$	$E_{yACOSH_i} :=$	$E_{yR1000_i} :=$	$E_{yR10000_i} :=$
.00001	.0476228 · μ	.010703 · μ	46.441 · n
.00002	.05293445 · μ	.016393 · μ	52.136 · n
.00004	.0595798 · μ	.023548 · μ	59.293 · n
.00006	.064302 · μ	.028659 · μ	64.406 · n
.00008	.0681337 · μ	.032826 · μ	68.573 · n
.00009	.06983764 · μ	.034684 · μ	70.432 · n
.0001	.071435755 · μ	.036431 · μ	72.178 · n
.0002	.08409979 · μ	.050399 · μ	86.146 · n
.0003	.0938388 · μ	.061313 · μ	97.059 · n
.0004	.10225 · μ	.070865 · μ	.10661 · μ
.0005	.1099038 · μ	.079655 · μ	.1154 · μ
.0006	.1184716 · μ	.087965 · μ	.12371 · μ
.00062	.11847164 · μ	.089585 · μ	.12533 · μ
.00064	.11847 · μ	.091193 · μ	.12694 · μ
.00066	.12122369 · μ	.09279 · μ	.12853 · μ
.00068	.1225845 · μ	.094377 · μ	.13012 · μ
.0007	.1239362 · μ	.095955 · μ	.1317 · μ
.00072	.1252794 · μ	.097523 · μ	.13327 · μ
.00074	.1266148 · μ	.099083 · μ	.13483 · μ
.00076	.129265 · μ	.10064 · μ	.13638 · μ
.00078	.12926475 · μ	.10218 · μ	.13792 · μ
.0008	.1305834 · μ	.10372 · μ	.13946 · μ
.0009	.137084 · μ	.11132 · μ	.14706 · μ
.001	.143501 · μ	.11879 · μ	.15454 · μ
.0011	.1498743 · μ	.12618 · μ	.16192 · μ
.0012	.156238 · μ	.13348 · μ	.16923 · μ
.0013	.1626233 · μ	.14074 · μ	.17648 · μ
.0014	.1690554 · μ	.14794 · μ	.18368 · μ
.0016	.182158 · μ	.16277 · μ	.19801 · μ
.0018	.19573196 · μ	.1765 · μ	.21224 · μ
.002	.209961 · μ	.19069 · μ	.22643 · μ
.0022	.2250453 · μ	.20489 · μ	.24063 · μ
.0024	.24121558 · μ	.21912 · μ	.25486 · μ
.0026	.25875145 · μ	.2334 · μ	.26915 · μ
.0028	.27800538 · μ	.24777 · μ	.28351 · μ
.003	.2994836 · μ	.26221 · μ	.29796 · μ
.004	.4745986 · μ	.33561 · μ	.37136 · μ
.005	.5 · μ	.40862 · μ	.44439 · μ
.006	.5 · μ	.47439 · μ	.51018 · μ
.007	.5 · μ	.52164 · μ	.55739 · μ
.008	.5 · μ	.53585 · μ	.57134134 · μ
.009	.5 · μ	.50224 · μ	.5362 · μ

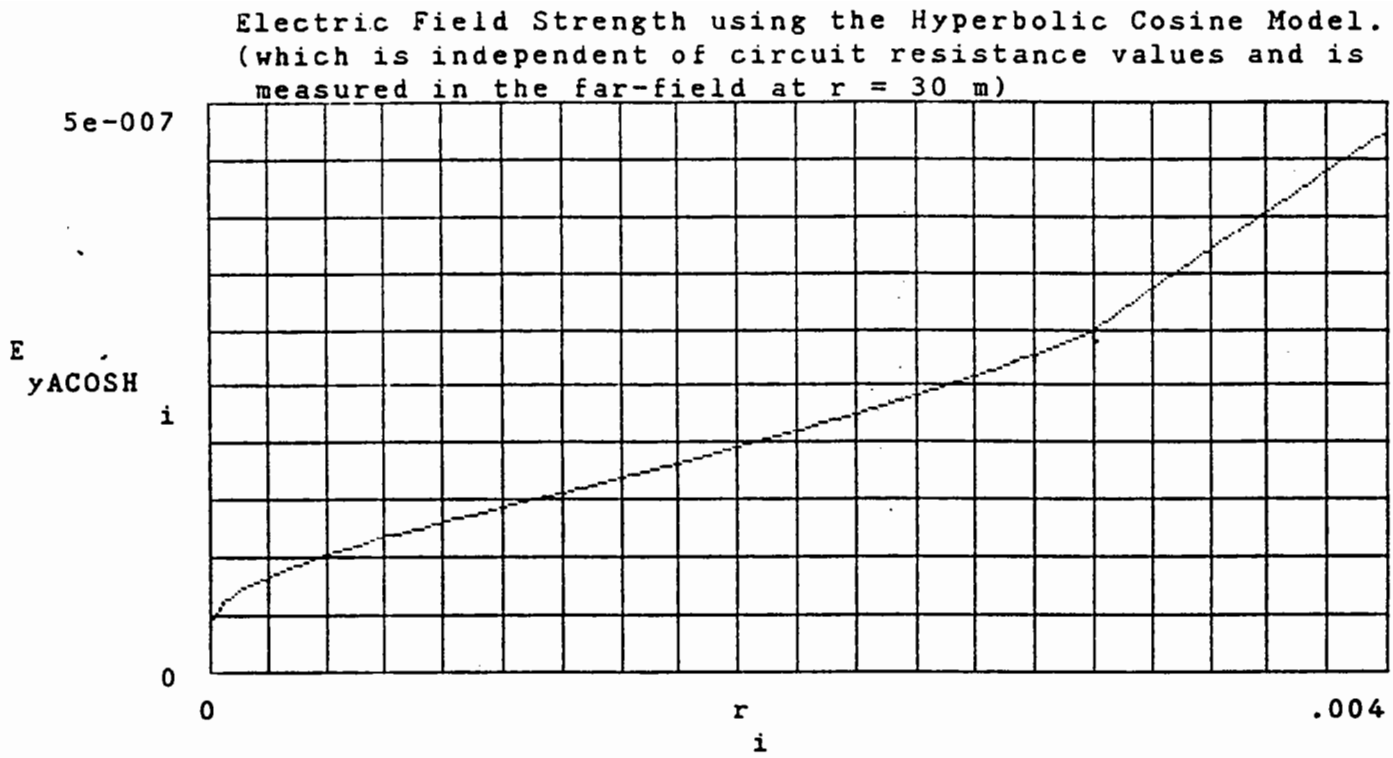

Horozontal Scale is .2 msec / div.

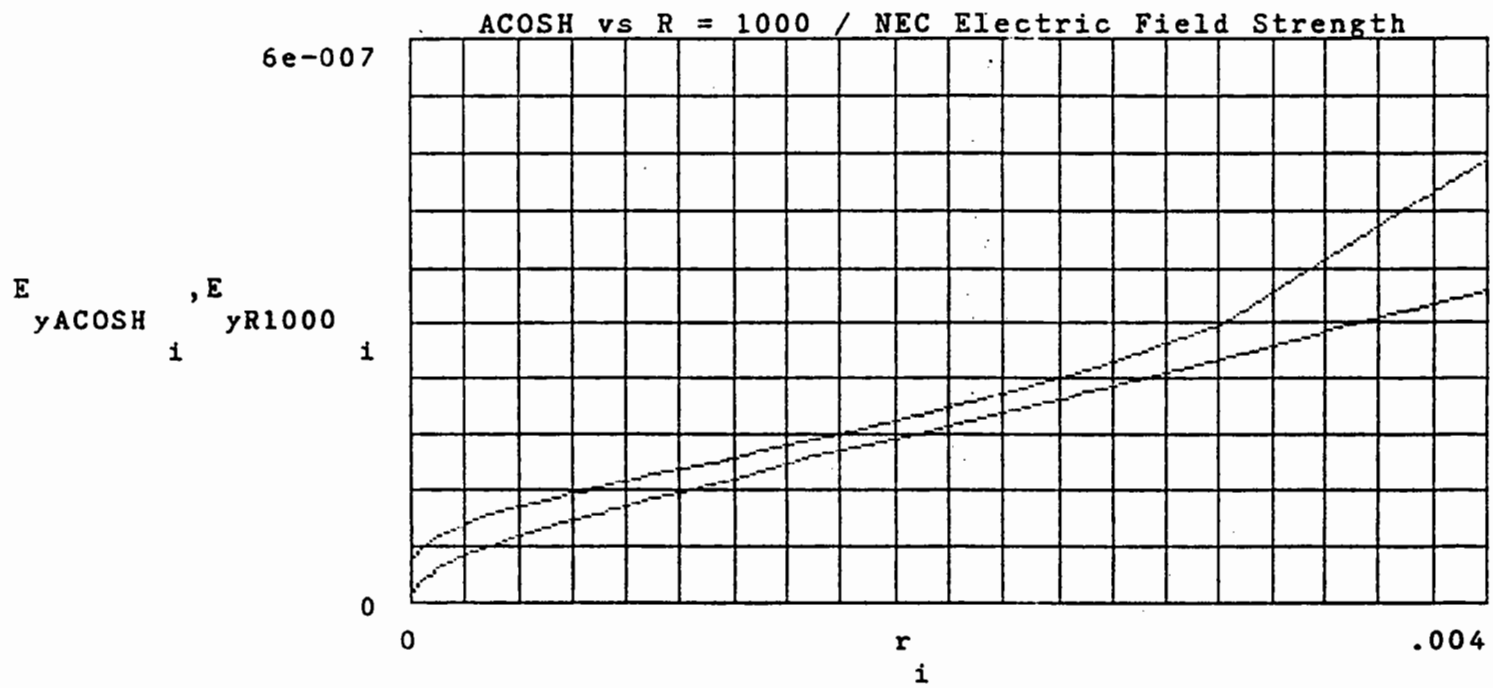

Horozontal Scale is .2 msec / div.

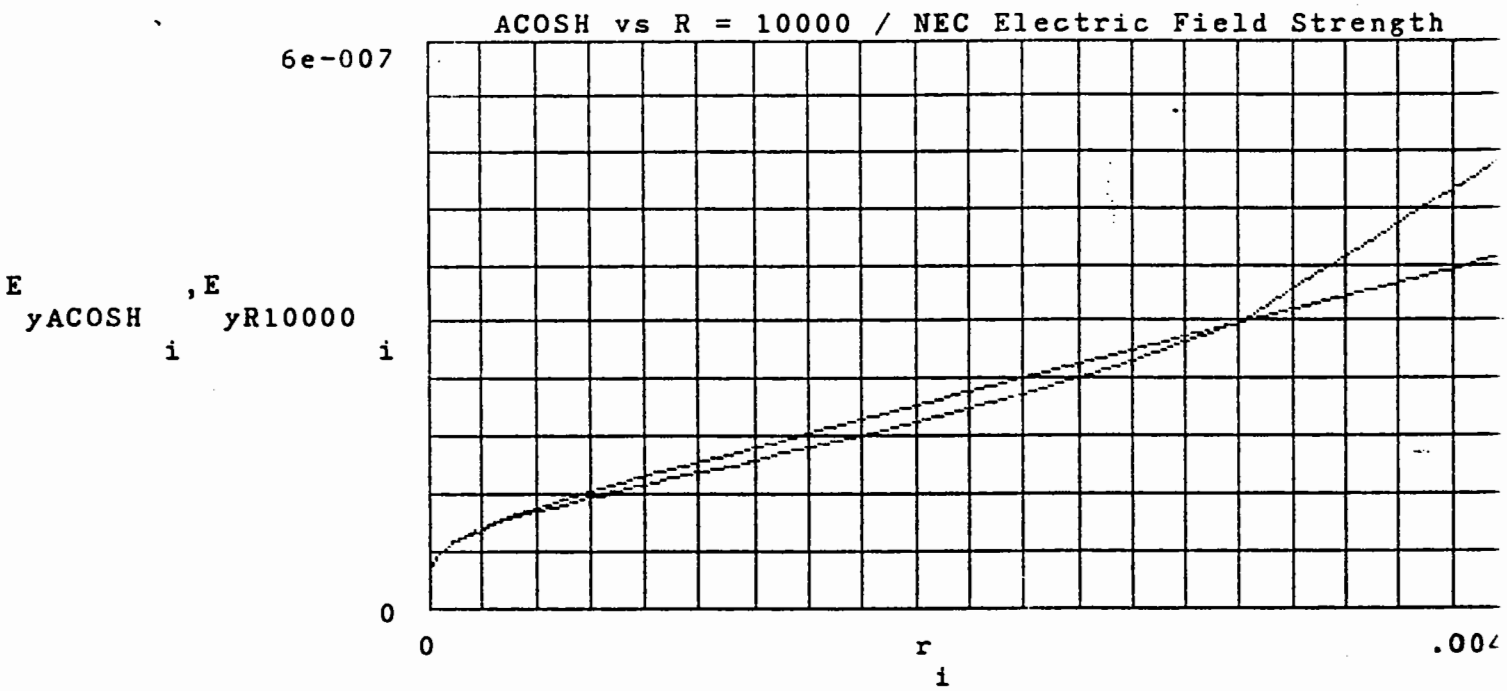

Horozontal Scale is .2 msec / div.

Plot of all the E-Fields combined. Includes the Ey-Field strengths for the circuits for R = 25Ω, R = 50Ω, R = 100Ω, R = 1 KΩ, and R = 10 KΩ.

$\mu \equiv 1 \cdot 10^{-6}$ $\quad n \equiv 1 \cdot 10^{-9}$ $\quad i := 0 \,..\, 41$

r := i	E yR25 := i	E yR50 := i	E yR100 := i	E yR1000 := i	E yR10000 := i
.00001	.83·μ	.57·μ	.3·μ	.010703·μ	46.441·n
.00002	.83·μ	.57·μ	.3·μ	.016393·μ	52.136·n
.00004	.83·μ	.57·μ	.3·μ	.023548·μ	59.293·n
.00006	.83·μ	.57·μ	.3·μ	.028659·μ	64.406·n
.00008	.83·μ	.57·μ	.3·μ	.032826·μ	68.573·n
.00009	.83069·μ	.57242·μ	.30142·μ	.034684·μ	70.432·n
.0001	.84339·μ	.57591·μ	.30066·μ	.036431·μ	72.178·n
.0002	.93391·μ	.59629·μ	.29277·μ	.050399·μ	86.146·n
.0003	.99207·μ	.60499·μ	.28501·μ	.061313·μ	97.059·n
.0004	1.035·μ	.60889·μ	.27749·μ	.070865·μ	.10661·μ
.0005	1.0687·μ	.61016·μ	.27016·μ	.079655·μ	.1154·μ
.0006	1.096·μ	.60974·μ	.26296·μ	.087965·μ	.12371·μ
.00062	1.1008·μ	.60951·μ	.26153·μ	.089585·μ	.12533·μ
.00064	1.1055·μ	.60923·μ	.2601·μ	.091193·μ	.12694·μ
.00066	1.11·μ	.60891·μ	.25868·μ	.09279·μ	.12853·μ
.00068	1.1144·μ	.60855·μ	.25726·μ	.094377·μ	.13012·μ
.0007	1.1186·μ	.60816·μ	.25584·μ	.095955·μ	.1317·μ
.00072	1.1226·μ	.60773·μ	.25442·μ	.097523·μ	.13327·μ
.00074	1.1265·μ	.60727·μ	.25301·μ	.099083·μ	.13483·μ
.00076	1.1303·μ	.60678·μ	.2516·μ	.10064·μ	.13638·μ
.00078	1.1339·μ	.60626·μ	.25019·μ	.10218·μ	.13792·μ
.0008	1.1374·μ	.60571·μ	.24878·μ	.10372·μ	.13946·μ
.0009	1.1533·μ	.60260·μ	.24177·μ	.11132·μ	.14706·μ
.001	1.1666·μ	.59897·μ	.23478·μ	.11879·μ	.15454·μ
.0011	1.1779·μ	.59491·μ	.22782·μ	.12618·μ	.16192·μ
.0012	1.1873·μ	.5905·μ	.22087·μ	.13348·μ	.16923·μ
.0013	1.1952·μ	.5855·μ	.21393·μ	.14074·μ	.17648·μ
.0014	1.2018·μ	.58085·μ	.207·μ	.14794·μ	.18368·μ
.0016	1.2115·μ	.57034·μ	.19312·μ	.16277·μ	.19801·μ
.0018	1.2174·μ	.55919·μ	.17925·μ	.1765·μ	.21224·μ
.002	1.2203·μ	.54752·μ	.16534·μ	.19069·μ	.22643·μ
.0022	1.2208·μ	.53544·μ	.15139·μ	.20489·μ	.24063·μ
.0024	1.2193·μ	.52299·μ	.13736·μ	.21912·μ	.25486·μ
.0026	1.2161·μ	.51023·μ	.12324·μ	.2334·μ	.26915·μ
.0028	1.2115·μ	.49718·μ	.10903·μ	.24777·μ	.28351·μ
.003	1.2057·μ	.48387·μ	.094709·μ	.26221·μ	.29796·μ
.004	1.1633·μ	.4145·μ	.021976·μ	.33561·μ	.37136·μ
.005	1.1091·μ	.34411·μ	.051433·μ	.40862·μ	.44439·μ
.006	1.0563·μ	.28123·μ	.11749·μ	.47439·μ	.51018·μ
.007	1.0209·μ	.24097·μ	.16692·μ	.52164·μ	.55739·μ
.008	1.0248·μ	.24902·μ	.19148·μ	.53585·μ	.57134134·
.009	1.1043·μ	.34432·μ	.20887·μ	.50224·μ	.5362·μ

$D2_i := E_{yR25_i}$ $D3_i := E_{yR50_i}$ $D4_i := E_{yR100_i}$

$D5_i := E_{yR1000_i}$ $D6_i := E_{yR10000_i}$

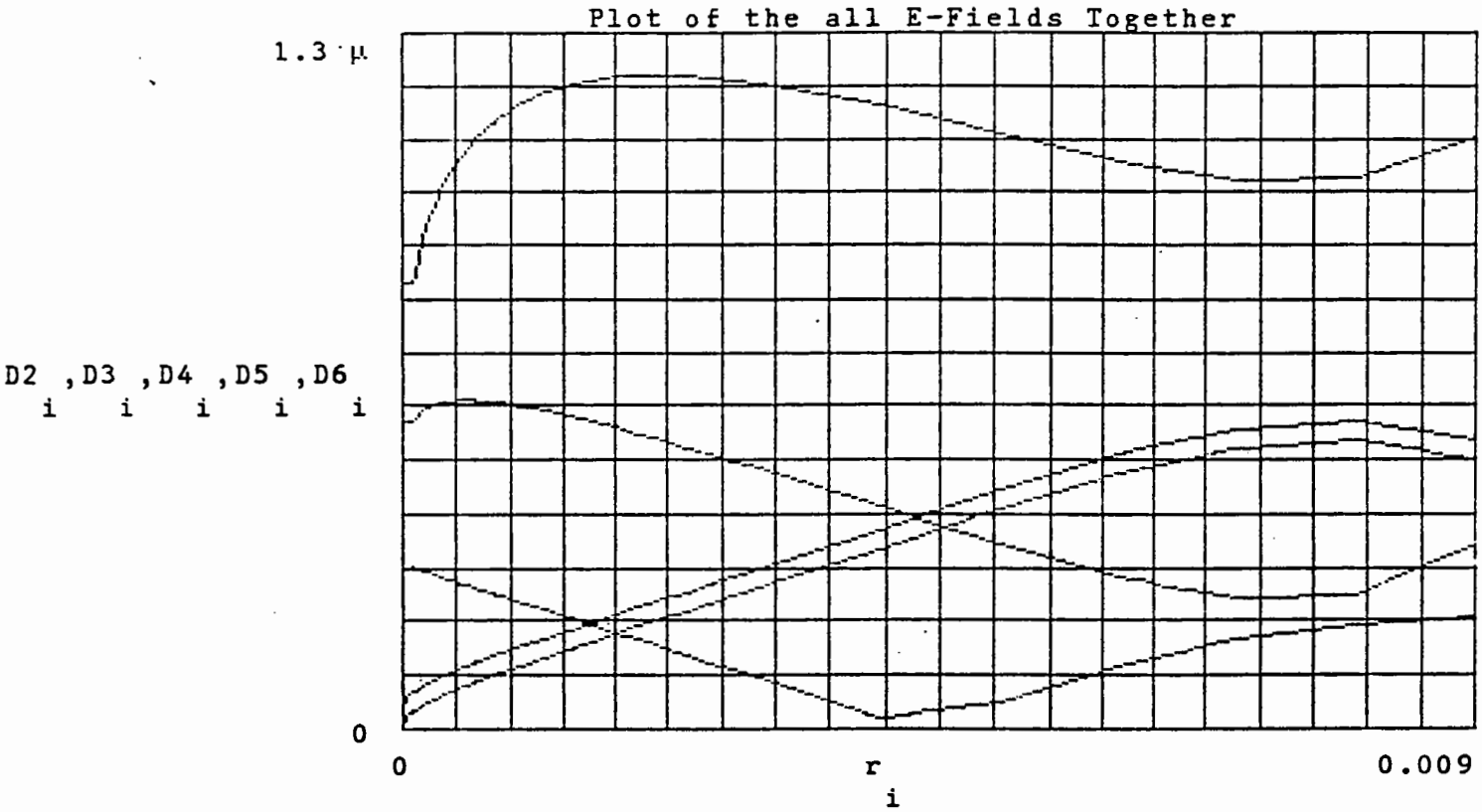

Horozontal scale is .45 m / div.

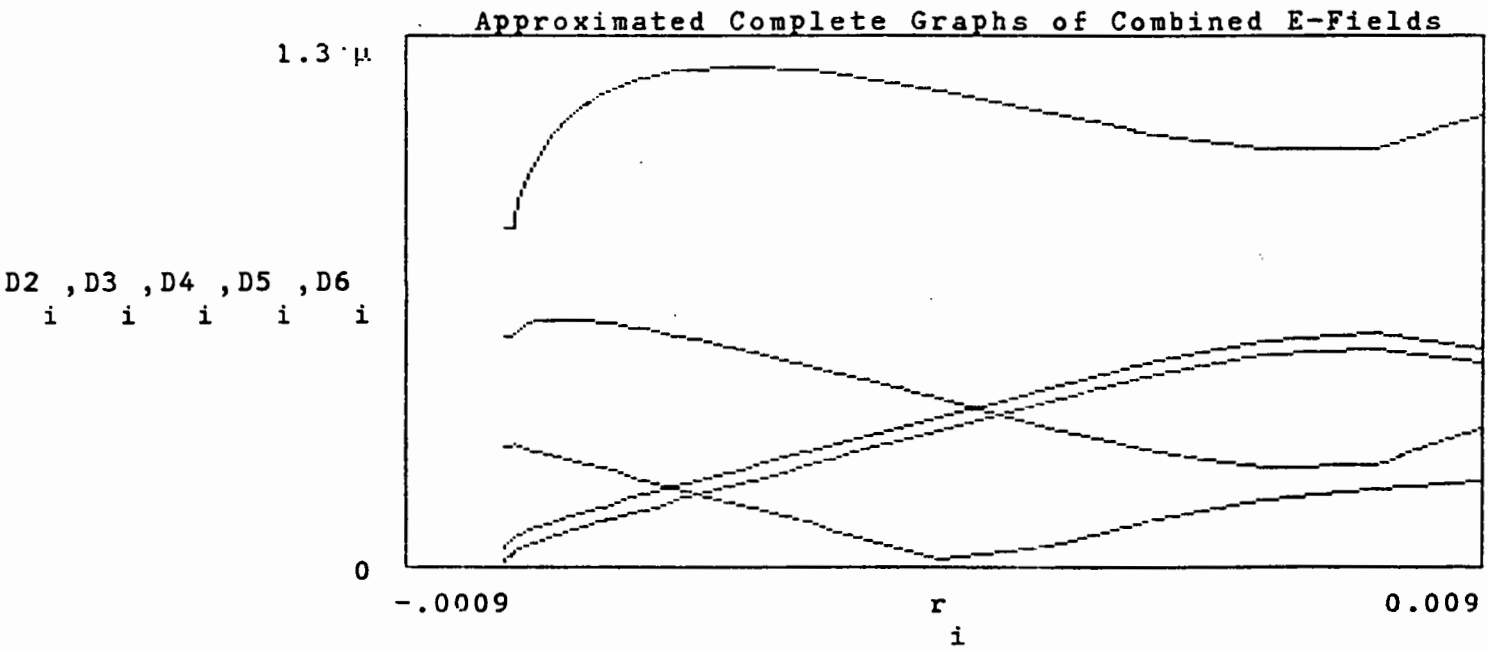

APPENDIX B

Development for:

$$|E|_{max}(R_L>\eta_o) = \frac{V\Delta S\beta^2}{(4r)\,acosh[\frac{\Delta z}{2a}]}$$

Given the circuit:

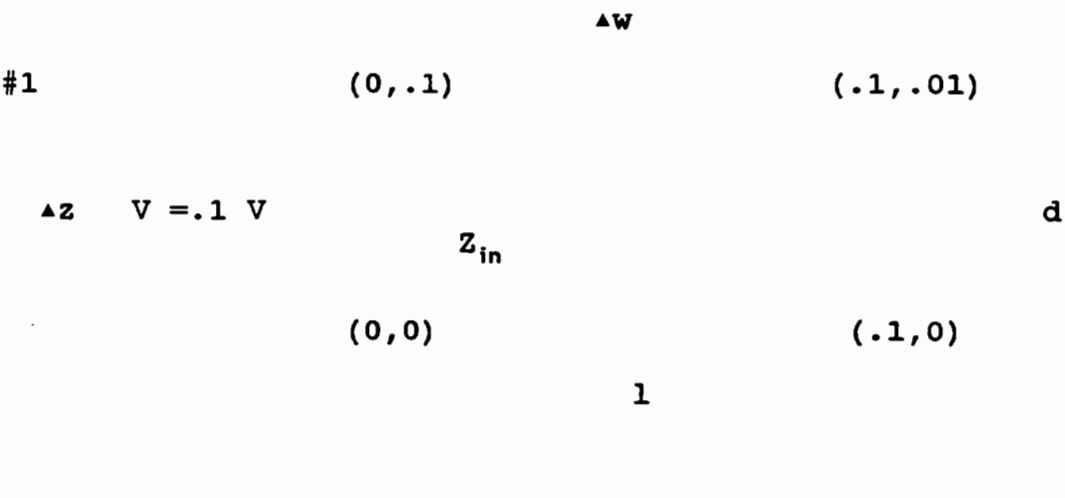

FIGURE #1

l = .1m f = 30 MHz wavelength = 10m

$$\lambda=\frac{C}{f}$$

$$\lambda=10m$$

$$\beta=\frac{2\pi}{\lambda}$$

$$\beta=.628$$

$$Z_i=Z_o[\frac{Z_L+jZ_o\tan\beta l}{Z_o+jZ_L\tan\beta l}]$$

note that:

$$\tan\beta l = .001096$$

$$\Delta S = \Delta z(\Delta w)$$

$$\Delta S = .001 m^2$$

where ▲S is the loop area

thus

$$\tan\beta l \approx \Delta w \beta$$

with

$$Z_L = \infty$$

$$\beta l = (.1)(.6283)$$

$$\beta l = .06283$$

because

$$\tan\beta l \approx \beta \Delta w$$

$$\Delta w = \frac{\lambda}{100}$$

$$\beta \Delta w = \left(\frac{2\pi}{\lambda}\right)\left(\frac{\lambda}{100}\right)$$

$$\beta \Delta w = .062831$$

and in radian measure

thus

$$\tan\beta l = .062913$$

$$\tan\beta l \approx \beta \Delta w$$

Now, in finding Z_{in}

$$Z_i = Z_o\left[\frac{\infty + jZ_o(\beta\Delta w)}{Z_o + j\infty(\beta\Delta w)}\right]$$

$$Z_i = Z_o\left[\frac{\infty}{\infty}\right]$$

Infinity over infinity is undefined and not possible. Applying L'Hopital's rule results in

$$Z_i = \lim\left[Z_o\left(\frac{\frac{d}{dZ_L}[Z_L + jZ_o\tan\beta l]}{\frac{d}{dZ_L}[Z_o + jZ_L\tan\beta l]}\right)\right]$$

$$Z_i = Z_o \lim\left[\frac{1+0}{0 + j\tan\beta l}\right]$$

$$Z_i = Z_o\left(\frac{1}{j\tan\beta l}\right)$$

$$Z_i = \frac{Z_o}{j\beta\Delta w}$$

$$|Z_i| = \frac{Z_o}{\beta\Delta w}$$

Using Z_o given in **Engineering Electromagnetics** by William H. Hayt, Jr., equation #12-30:

and

$$Z_o = \frac{1}{\pi}\sqrt{\frac{\mu_o}{e_o}}\,acosh\left[\frac{d}{2a}\right]$$

$$E_\theta = \frac{I\Delta z \eta_o \beta}{4\pi r}$$

$$I = \frac{V}{|Z_1|}$$

$$|Z_1| = \frac{\left[\frac{1}{\pi}\sqrt{\frac{\mu_o}{e_o}}\,acosh\left[\frac{d}{2a}\right]\right]}{\beta\Delta w}$$

$$I = \frac{V\beta\Delta w}{\frac{1}{\pi}\sqrt{\frac{\eta_o}{e_o}}\,acosh\left[\frac{d}{2a}\right]}$$

$$E_\theta = \frac{\left[\frac{V\beta\Delta w}{\frac{1}{\pi}\sqrt{\frac{\mu_o}{e_o}}\,acosh\left[\frac{d}{2a}\right]}\right]\Delta z \eta_o \beta}{4\pi r}$$

$$E_\theta = \frac{V\Delta S \eta_o \beta^2 \pi}{4\pi r \eta_o\, acosh\left[\frac{d}{2a}\right]}$$

resulting in

$$|E_\theta| = \frac{V\Delta S\beta^2}{4r\,acosh\left[\frac{d}{2a}\right]}$$

for $R_L > 377\Omega$

where

a = wire radius
b = wire separation
V = forcing function in V_{peak}
r = far field distance

Development for:

$$E_\theta = \frac{V\Delta S\eta_o\beta^2}{4\pi r\sqrt{R^2+[2\pi f(\frac{\mu_o}{e_o})\,acosh[\Delta\frac{z}{2a}]]^2}}$$

for values of $R_L < 377\Omega$

Using figure #1

$$Y_i = \frac{1}{Z_i}$$

$$I = \frac{V}{Z_i}$$

$$I = V(Y_i)$$

it is easy to see here that with a scaling factor V the input admittance, Y_{in}, represents the antenna current.

$$Z_i = R_L + j\omega L$$

$$Y_i = \frac{1}{R_L + j\omega L}$$

here L equals the external inductance, L_{ext}:

$$L_{ext} = \frac{\mu_o}{\pi} acosh[\frac{d}{2a}]$$

or

$$L=\frac{\mu_o}{\pi}acosh[\frac{\Delta z}{2a}]$$

$$Z_1=R+j\omega[\frac{\mu_o}{\pi}acosh[\frac{\Delta z}{2a}]]$$

$$|Z_1|=\sqrt{R^2+[2\pi f\frac{\mu_o}{\pi}acosh[\frac{\Delta z}{2a}]]^2}$$

The dual of the electric loop is the magnetic dipole. This results in:

$$E_\phi=\frac{I\Delta S\eta_o\beta^2}{4\pi r}$$

subbing in

$$I=\frac{V}{|Z_1|}$$

subbing for I and Z_{in}

$$E_\phi=\frac{V\Delta S\eta_o\beta^2}{4\pi r\sqrt{R^2+[2\pi f\frac{\mu_o}{\pi}acosh[\frac{\Delta z}{2a}]]^2}}$$

for values of R_L < 377Ω

APPENDIX C

Experimental Testing Data and Plots

The experimental verification phase involve connecting up three loop antennas of wire radiuses:

$$r \approx .45mm$$

This corresponds to r = .4mm and Y_{in} = .0159577 - j.00793974 S NEC calculated values.

$$r \approx 1.3mm$$

This corresponds to r = 1.3mm and Y_{in} = .0183257 - j.00538704 S NEC calculated values.

$$r \approx 2.05mm$$

This corresponds to r = 2mm and Y_{in} = .018972 - j.0042166 S NEC calculated values.

The three loop antennas were made of copper wire and shaped in a 1cm x 10cm rectangle with one end open (see figure #11). The antennas were connected to the network analyzer (N.A.) by a Z_o = 50Ω coaxial cable. A BNC connector was mated to the S_{11} port of the N.A. with the end connected to the antenna made with alligator clips.

FIGURE A

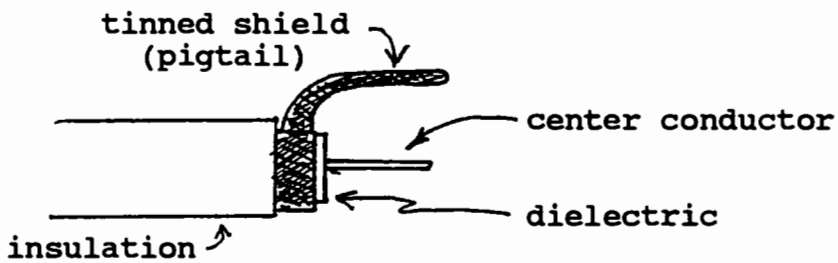

The end of the coax cable connected to the loop antenna was configured as in figure A. The coax was connected to the antenna as

close as possible to reduce loop area. The only effective loop area was within the loop antenna itself.

Although the preferred interconnecting cable, the 50Ω coax, was not the first used. After steps to calibrate the N.A., a BNC to banana lead cable was used to connect the antennas to the N.A.

FIGURE B

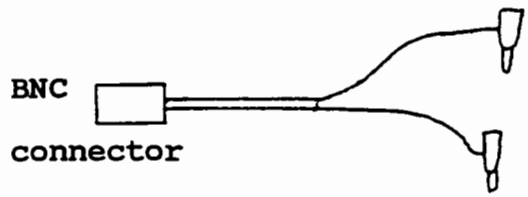

When measured, the reflection coefficient, Γ, read

$$\Gamma=1.458\angle 154.73^{\circ}$$

as given in Plot AA for the loop of radius 1.3mm. This was an erroneous reading since Γ_{max} should only equal one. 1.458 means the N.A. was receiving more than just reflected power. The loop was acting as a source. The loop of the banana clips was larger than the loop of the antenna. For this reason, the switch to the coax was made to achieve more accurate results.

Using the coax cable with the N.A., the expected measured values should have come close to the NEC values for Γ.

For NEC:

$$r=.4mm$$

$$Z_i=50.23+j24.99\Omega$$

$$\Gamma=.242\angle 75.5^{\circ}$$

r=1.3mm

Z_i=50.23+j14.77Ω

Γ=.146∠80.7°

The values returned by the N.A.:

r=.45mm

Z_i=359.4-j1319Ω

Γ=.981∠-4.04°

r=1.3mm

Z_i=-1.294-j10.093Ω

Γ=1.051∠157.16°

The expected values for Γ were to have a magnitude less than one and a phase in the vicinity 90°. As can be seen with the plots and calculations, the measured and expected values were not even close. A problem in measurement existed again. This time the loop inductance could not be the problem because of the test circuit configuration. The calibration procedure was then in question.

Calibration was performed to make the cable part of the test set. Meaning, the open end, as in figure A, is not an open to the N.A. (capacitive), but reference zero. When calibrated, the open

ended cable read zero magnitude and phase. To do this, three standards were used. Cable open ended, cable shorted, and cable replaced with a precision 50Ω load.

When the three antennas were measured, the results were plotted and given as Plots #1A, #1B, and #1C. Γ was calculated and for the small loop, was .981 at an angle of 157°. With the second loop, Γ has a magnitude greater than one and nearly twice the phase of the expected value. The magnitude greater than one results in Z_{in} with a negative real part. Negative resistance does not exist. It became obvious, improvements in the calibration procedures were necessary.

A change in the calibration was tried. The open and short cal-methods were done as before, but the precision 50Ω load was calibrated at the cable end. This produced results taking the form of Plots #2A, #2B, and #2C. At this point, the reflection coefficients were all less than one, but the phase was still off.

The calibration procedures followed were those outlined in the Quick Reference Guide of the HP-8753 Network Analyzer. They were followed and the N.A. responded as if the procedure was done correctly. If any step, open - short - load, was skipped the N.A. responded by asking for additional standards.

In the reference manual for the N.A., page 5-21, there is a slightly different calibration procedure. This was attempted and the N.A. rejected this calibration technique. It required additional standards. It is clear the calibration procedures must be established and eliminated before answers as to why the measured

results do not match the expected results can be found.

Plot # AA

(1.458) Lineal conversion

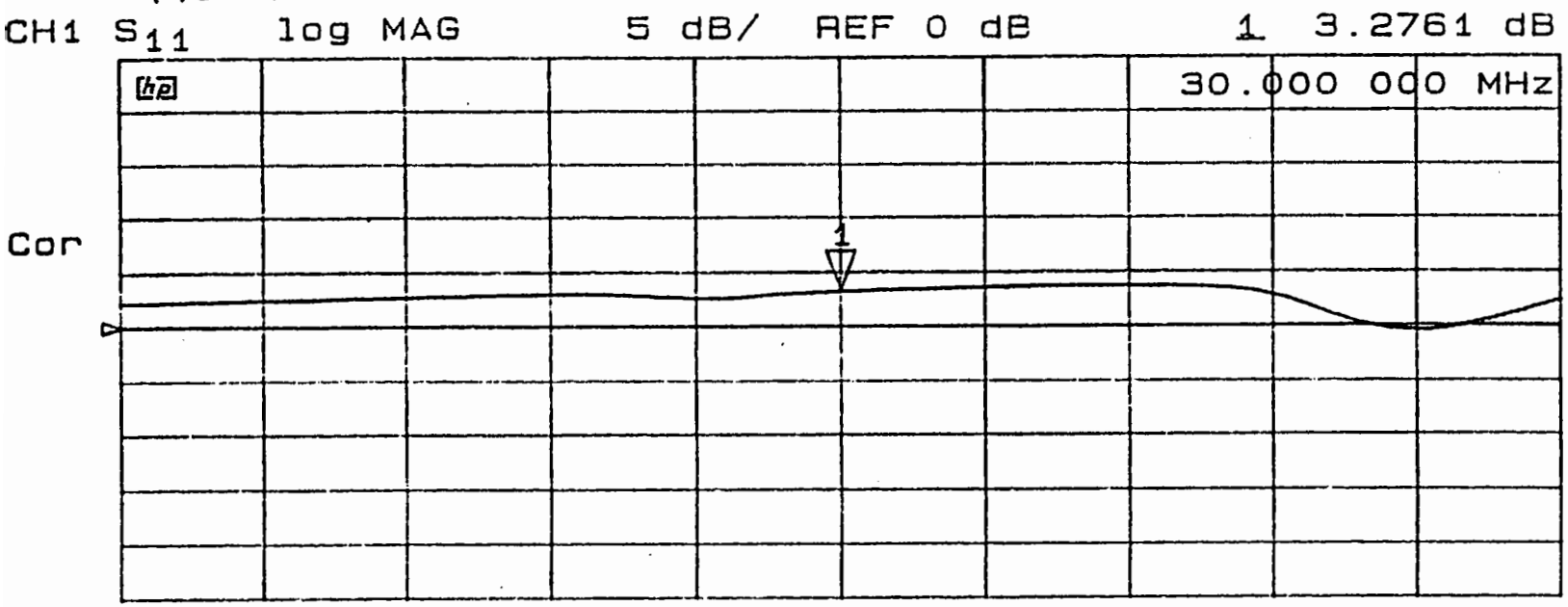

System Calibrated with bannana lead cable {excessive loop area}

R= 1.3mm

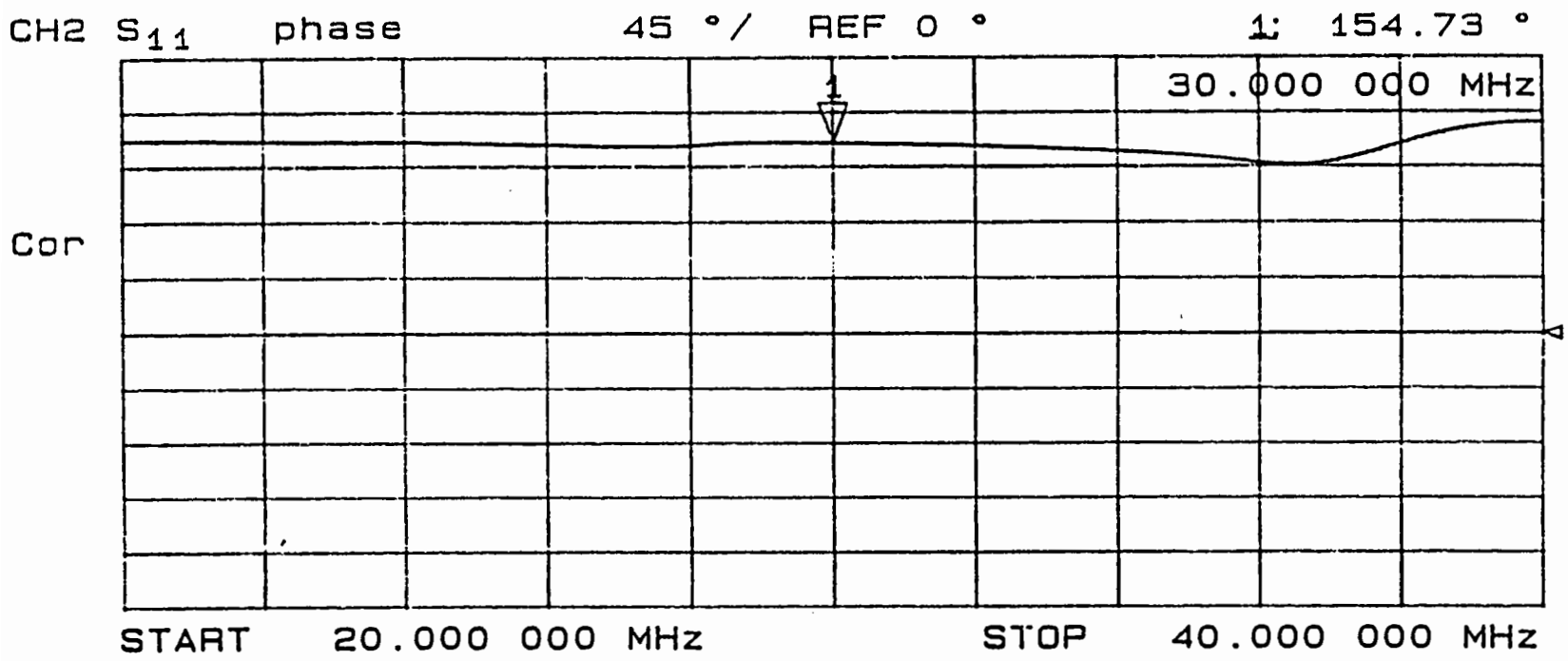

#1B

(1.051)← conversion to Linear

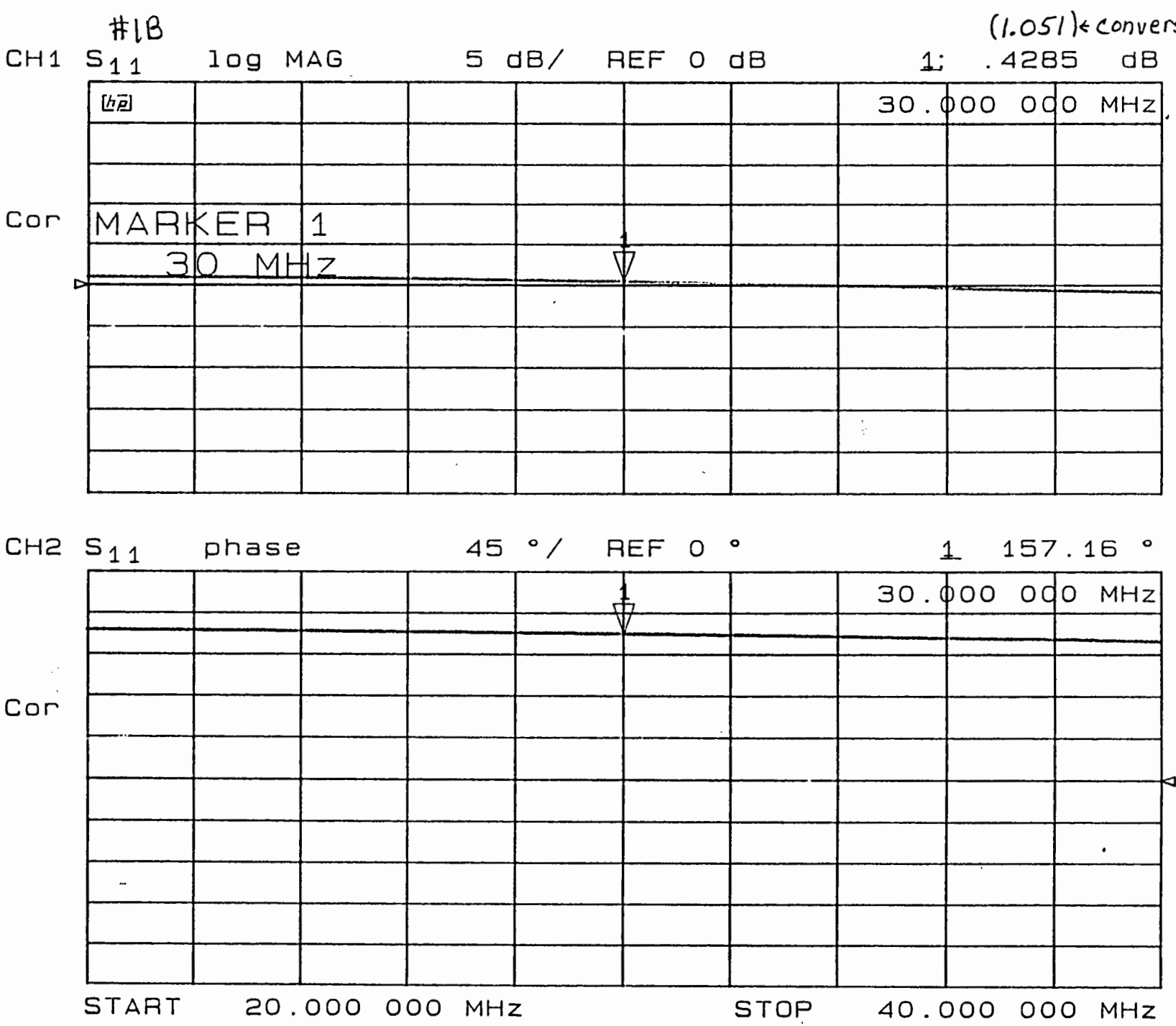

wire Radius ≈ 1.3mm

#2

#1C

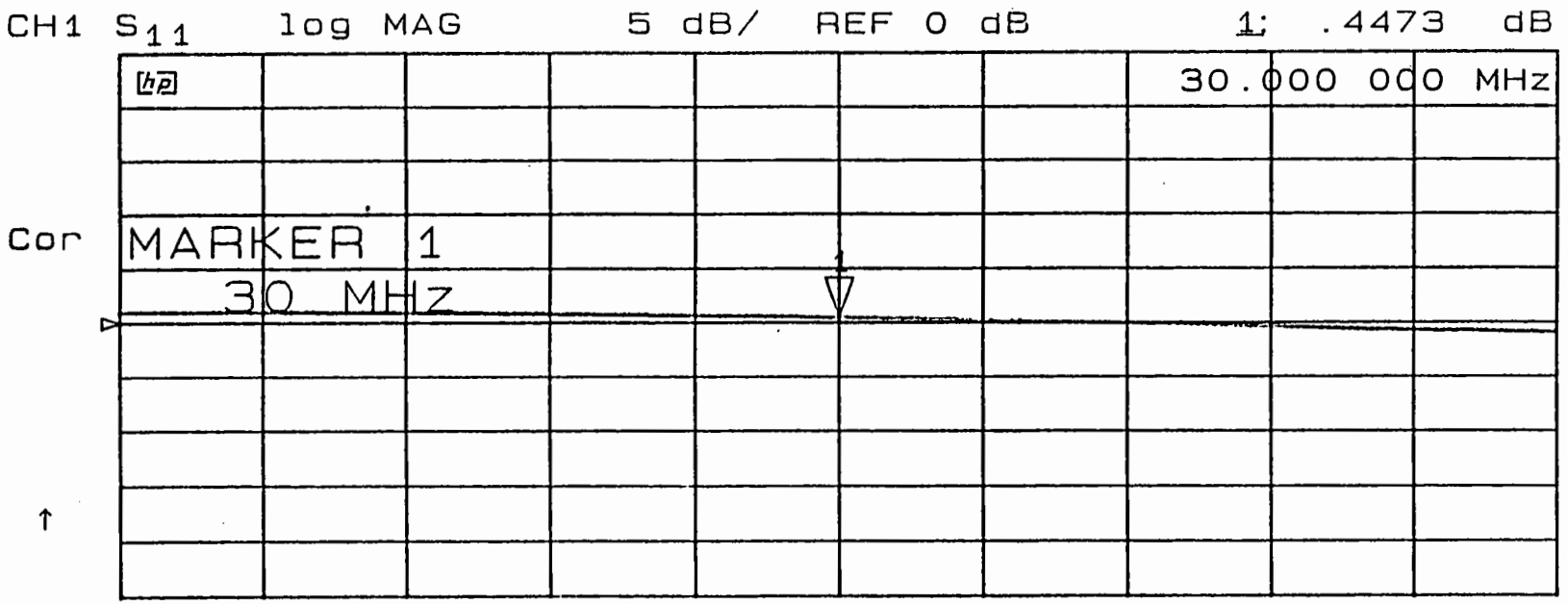

Wire
Radius ≅ .00205 m

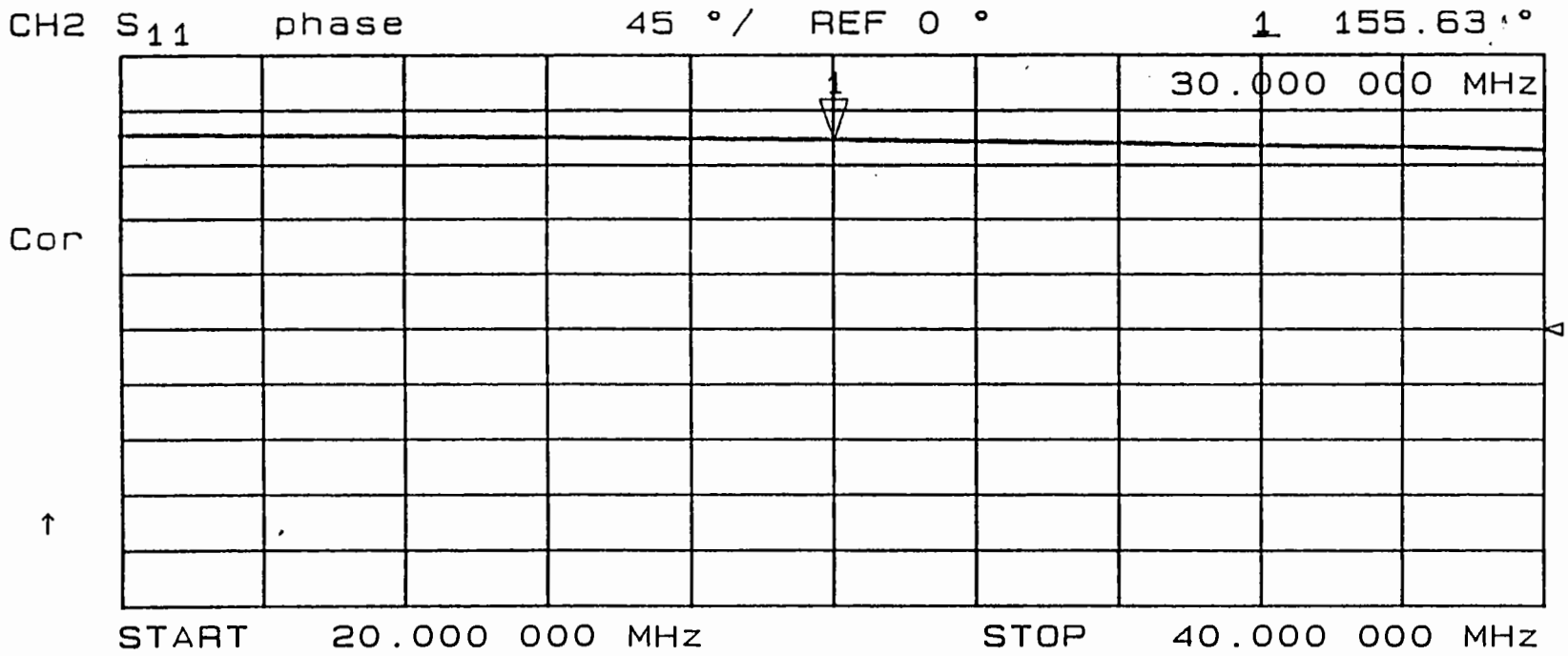

#3

#2A {Load Calibrated at cable end.}

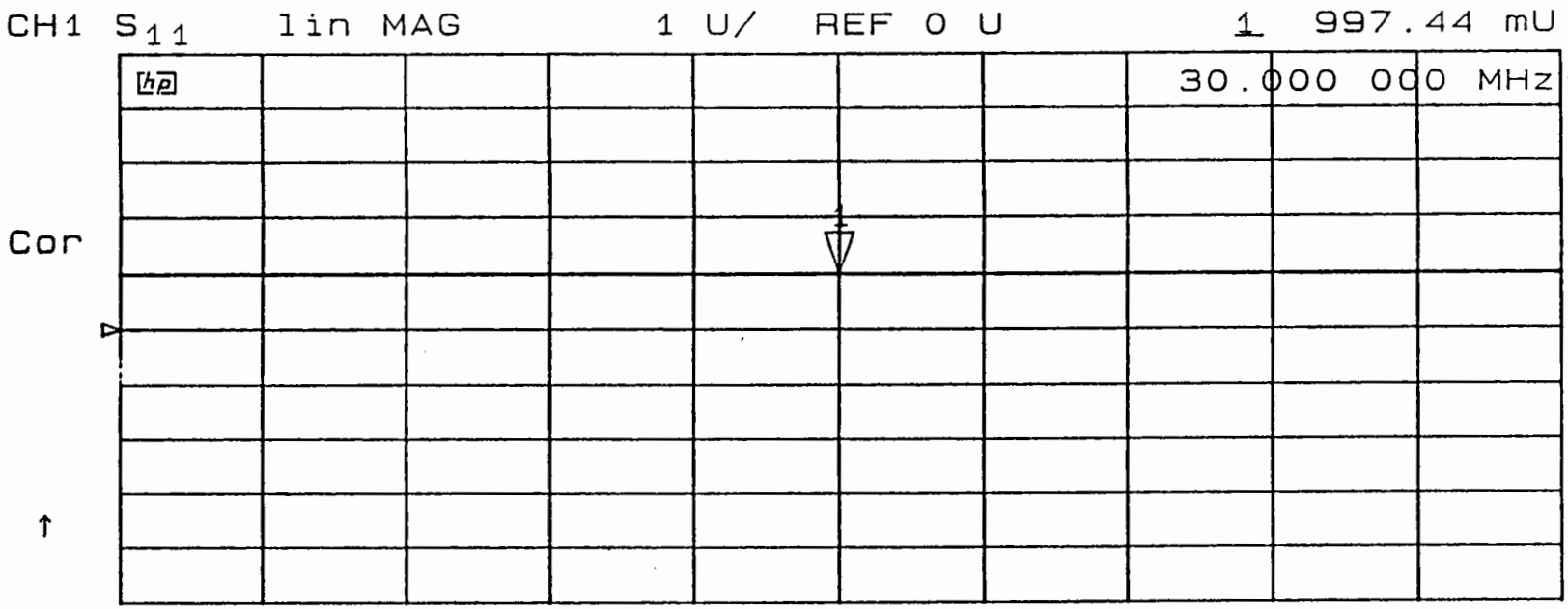

wire
Radius = .45mm

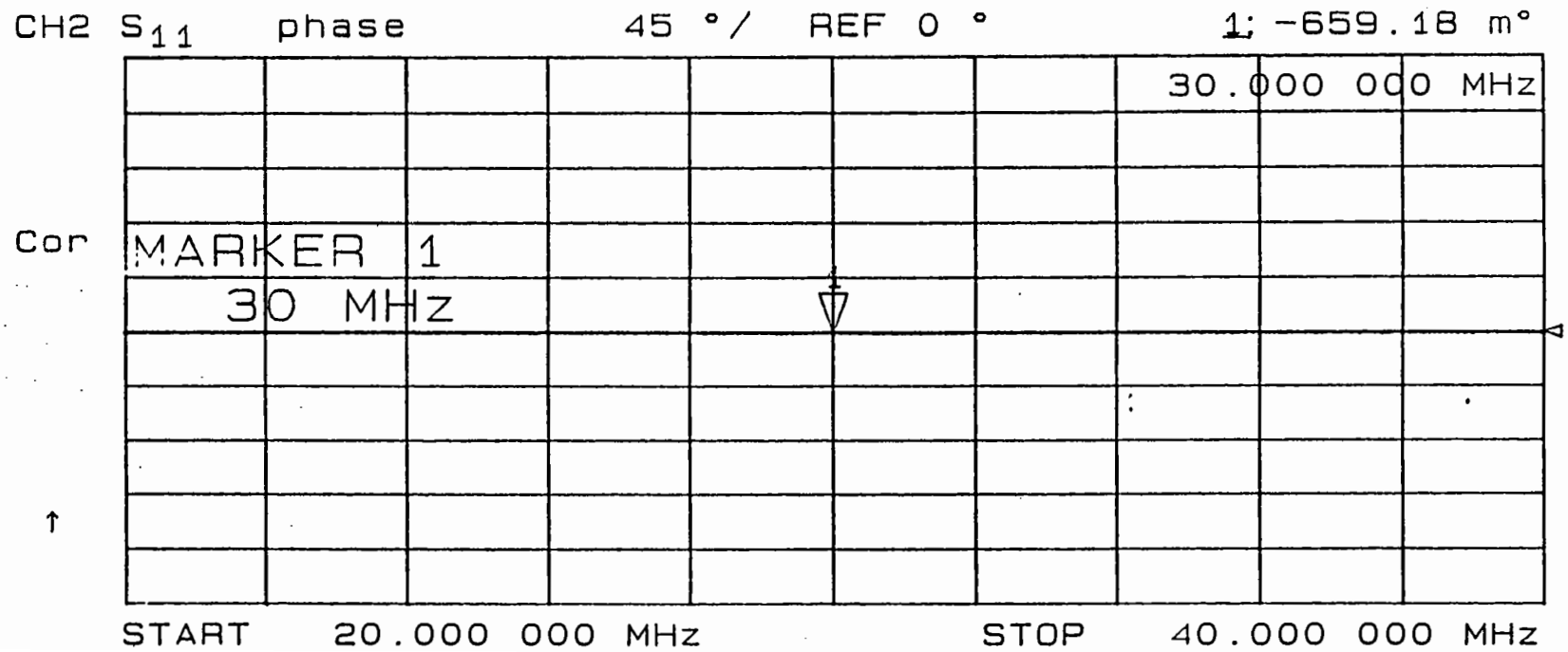

#2C

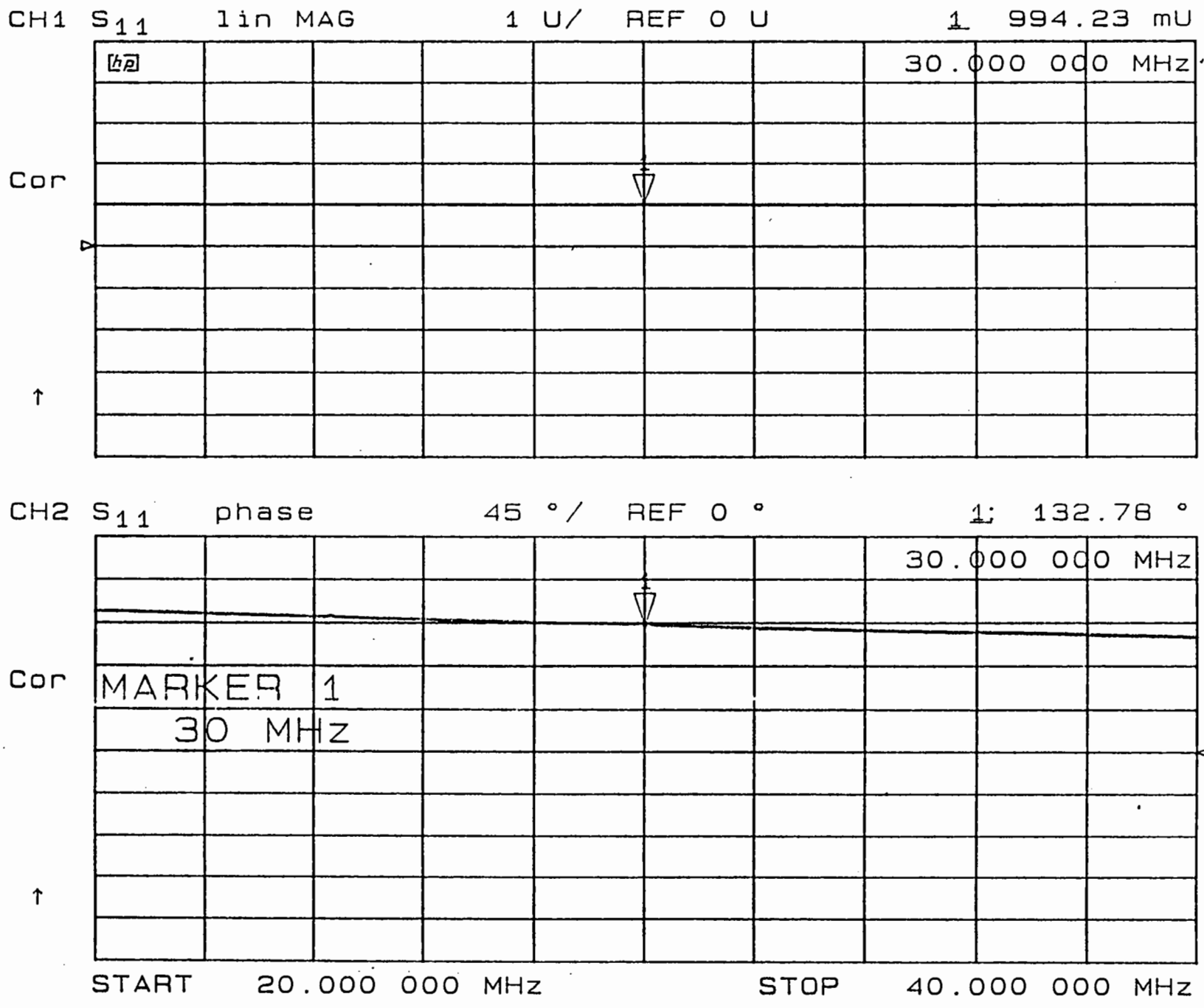

Large Loop.

Wire
Radius = 2.05 mm

#1 R = 50 Ω | CALCULATIONS for Zin with Plot set #1

Γ = -.167 dB ∠ -4.04° Radius = .45 mm

= .981 ∠ -4.04°

= .9786 - j.0691

$$\Gamma = \frac{Z_{in} - Z_o}{Z_{in} + Z_o}$$

where $Z_o = 50\ \Omega$

$$.9786 - j.0691 = \frac{Z_{in} - 50}{Z_{in} + 50}$$

$$(.9786 - j.0691)Z_{in} + 50(.9786 - j.0691) = Z_{in} - 50$$

$$Z_{in}(.9786 - j.0691) - Z_{in} = -50 - (48.93 - j3.46)$$

$$Z_{in}(.9786 - j.0691 - 1) = -98.928 + j3.456$$

$$Z_{in} = \frac{-98.928 + j3.456}{.9786 - j.0691}$$

$$Z_{in} = 359.4 - j1319$$

$$Y_{in} = \frac{1}{Z_{in}}$$

$$\boxed{Y_{in} = 1.921 \times 10^{-4} + j\,7.053 \times 10^{-4}\ \mho}$$

$$Y_{in_{\substack{R50\,NEC \\ (r=.0004)}}} = 1.59577 \times 10^{-2} - j\,7.93974 \times 10^{-3}$$

Values are not even close, but the Real part of Zin is positive.

#2 $R = 50\Omega$

$\Gamma = +.4285\,dB \angle 157.16^\circ$ Radius = 1.3mm

$= 1.051 \angle 157.16^\circ$

$\Gamma = -.9686 + j.40796$

$$\Gamma = \frac{Z_{in} - Z_o}{Z_{in} + Z_o}$$

$$-.9686 + j.40796 = \frac{Z_{in} - 50}{Z_{in} + 50}$$

$(-.9686 + j.40796)(Z_{in} + 50) = Z_{in} - 50$

$Z_{in}(-.9686 + j.4079) + 50(-.9686 + j.4079) = Z_{in} - 50$

$Z_{in}(-.9686 + j.40796) + 50(-.9686 + j.40796) = Z_{in} - 50$

$Z_{in}(-.9686 + j.40796) - Z_{in} = -50 - (-48.43 + j20.398)$

$Z_{in}(-.9686 + j.4079 - 1) = -1.5703 - j20.398$

$$Z_{in} = \frac{-1.5703 - j20.398}{-1.9686 + j.40796}$$

$\boxed{Z_{in} = -1.294 + j10.093\,\Omega}$ ok

$$Y_{in} = \frac{1}{Z_{in}}$$

$Y_{in} =$

$Y_{in_{RSONEC}} = 1.83257 \times 10^{-2} - j5.38704 \times 10^{-3}$
$(r = .0013)$

$$\%d = \left|\frac{NEC - meas.}{NEC}\right| (100\%)$$

#2 $R = 50\Omega$

$\Gamma = +.4285\,dB \angle -157.16^\circ$ Radius = 1.3mm

$= 1.051 \angle 157.16^\circ$

$\Gamma = -.9686 + j.40796$

$$\Gamma = \frac{Z_{in} - Z_o}{Z_{in} + Z_o}$$

$$-.9686 + j.40796 = \frac{Z_{in} - 50}{Z_{in} + 50}$$

$(-.9686 + j.40796)(Z_{in} + 50) = Z_{in} - 50$

$Z_{in}(-.9686 + j.4079) + 50(-.9686 + j.4079) = Z_{in} - 50$

$Z_{in}(-.9686 + j.40796) + 50(-.9686 + j.40796) = Z_{in} - 50$

$Z_{in}(-.9686 + j.40796) - Z_{in} = -50 - (-48.43 + j20.398)$

$Z_{in}(-.9686 + j.4079 - 1) = -1.5703 - j20.398$

$$Z_{in} = \frac{-1.5703 - j20.398}{-1.9686 + j.40796}$$

$\boxed{Z_{in} = -1.294 + j10.093\,\Omega}$ ok

$$Y_{in} = \frac{1}{Z_{in}}$$

$Y_{in} =$

$Y_{in_{RSONEC}} = 1.83257 \times 10^{-2} - j5.38704 \times 10^{-3}$
$(r = .0019)$

$$\%d = \left|\frac{NEC - meas.}{NEC}\right| (100\%)$$

ACKNOWLEDGEMENTS

[1] T. H. Hubing and J. F. Kaufman, **Modelling the Electromagnetic Radiation from Electrically Small Table Top Products.** IEEE Trans. EMC, vol 31, No. 1, February 1989, p.83.

[2] C. A. Balanis, **Antenna Theory, Analysis and Design.** Harper and Row, New York, 1982, p.58 and 170.

[3] T. H. Hubing and J. F. Kaufman, p. 74.

[4] T. H. Hubing and J. F. Kaufman, p. 82.

[5] W. H. Hayt, Jr., **Engineering Electromagnetics.** McGraw-Hill, 1981, p. 438.